A Novel Gene, *OZONE-RESPONSIVE APOPLASTIC PROTEIN1*, Enhances Cell Death in Ozone Stress in Rice[1]

Yoshiaki Ueda, Shahid Siddique, and Michael Frei*

Institute of Crop Science and Resource Conservation, Plant Nutrition (Y.U., M.F.) and Molecular Phytomedicine (S.S.), University of Bonn, 53115 Bonn, Germany

ORCID IDs: 0000-0002-4304-368X (Y.U.); 0000-0001-7503-4318 (S.S.); 0000-0002-2474-6558 (M.F.).

A novel protein, OZONE-RESPONSIVE APOPLASTIC PROTEIN1 (OsORAP1), was characterized, which was previously suggested as a candidate gene underlying *OzT9*, a quantitative trait locus for ozone stress tolerance in rice (*Oryza sativa*). The sequence of OsORAP1 was similar to that of ASCORBATE OXIDASE (AO) proteins. It was localized in the apoplast, as shown by transient expression of an OsORAP1/green fluorescent protein fusion construct in *Nicotiana benthamiana* leaf epidermal and mesophyll cells, but did not possess AO activity, as shown by heterologous expression of OsORAP1 in Arabidopsis (*Arabidopsis thaliana*) mutants with reduced background AO activity. A knockout rice line of *OsORAP1* showed enhanced tolerance to ozone stress (120 nL L^{-1} average daytime concentration, 20 d), as demonstrated by less formation of leaf visible symptoms (i.e. cell death), less lipid peroxidation, and lower NADPH oxidase activity, indicating reduced active production of reactive oxygen species. In contrast, the effect of ozone on chlorophyll content was not significantly different among the lines. These observations suggested that OsORAP1 specifically induced cell death in ozone stress. Significantly enhanced expression of jasmonic acid-responsive genes in the knockout line implied the involvement of the jasmonic acid pathway in symptom mitigation. Sequence analysis revealed extensive polymorphisms in the promoter region of *OsORAP1* between the ozone-susceptible cv Nipponbare and the ozone-tolerant cv Kasalath, the *OzT9* donor variety, which could be responsible for the differential regulation of *OsORAP1* reported earlier. These pieces of evidence suggested that OsORAP1 enhanced cell death in ozone stress, and its expression levels could explain the effect of a previously reported quantitative trait locus.

Tropospheric ozone is one of the most important environmental pollutants adversely affecting agriculture (Ainsworth et al., 2012). Ozone is formed through photochemical reactions of precursor gases such as nitrogen oxides, carbon monoxide, and volatile organic compounds, which largely originate from anthropogenic gas emissions (Yamaji et al., 2006). Recent economic development and industrialization have led to drastic increases of tropospheric ozone concentrations in East Asian countries. In some regions, the monthly average concentration currently exceeds 70 nL L^{-1} (Yamaji et al., 2006), temporarily reaching nearly 200 nL L^{-1} (Wang et al., 2007). Furthermore, the average level is expected to increase by up to 10 nL L^{-1} by 2020 in these areas compared with 2000, due to increasing anthropogenic gas emissions (Yamaji et al., 2008). At these concentrations, ozone negatively affects both crop yields (Ainsworth, 2008) and quality (Wang and Frei, 2011) and induces leaf visible symptoms such as chlorosis and bronzing (Feng et al., 2014).

Rice (*Oryza sativa*) is the major staple crop throughout Asia, and it is strongly affected by tropospheric ozone because its cropping season overlaps with peak ozone concentrations, especially in South and East Asia (Frei, 2015). Previous studies estimated around 3.7% of global rice yield loss and regionally more than 10% of rice yield loss due to elevated tropospheric ozone, and this trend will exacerbate in the future with increasing concentrations (Ainsworth, 2008; Van Dingenen et al., 2009). Considering that the global food demand will double by the year 2050 (Tilman et al., 2011), it is of paramount importance to get insight into ozone tolerance mechanisms in rice and breed ozone-tolerant rice varieties to ensure the global food supply.

A number of previous studies have determined genetic factors associated with ozone tolerance in rice, suggesting that this trait is controlled by multiple medium-effect loci rather than a single large-effect locus (Frei, 2015; Ueda et al., 2015). In a study by Frei et al. (2008), several ozone-related quantitative trait loci (QTLs) were identified using a mapping population

[1] This work was supported by the Deutsche Forschungsgemeinschaft (grant no. FR2952/1–1).

* Address correspondence to mfrei@uni-bonn.de.

The author responsible for distribution of materials integral to the findings presented in this article in accordance with the policy described in the Instructions for Authors (www.plantphysiol.org) is: Michael Frei (mfrei@uni-bonn.de).

Y.U. performed most of the experiments, analyzed the data, and wrote the article; S.S. designed the experiments, performed the confocal microscopy experiments, and contributed to the writing; M.F. conceived the original research plans, compiled and genotyped the rice mutants, designed and supervised the experiments, and contributed to the writing.

www.plantphysiol.org/cgi/doi/10.1104/pp.15.00956

derived from the contrasting cultivars Nipponbare (susceptible) and Kasalath (tolerant). One of the identified QTLs, *OzT9*, was related to leaf visible symptom formation in ozone stress, where the allele from the tolerant cv Kasalath conferred tolerance. Underpinning the effect of *OzT9*, a chromosomal segment substitution line, SL41, carrying a chromosomal introgression from cv Kasalath at the *OzT9* locus in the cv Nipponbare background, produced less visible symptoms than cv Nipponbare (Frei et al., 2008). A subsequent transcriptomic analysis revealed a differential gene expression profile between cv Nipponbare and SL41 (Frei et al., 2010). A proposed candidate gene, which was annotated as an ASCORBATE OXIDASE (AO; Rice Annotation Project Database [RAP-DB] identifier *Os09g0365900*), was located near the *OzT9* locus and was one of the most highly induced genes in ozone stress in the whole array. The induction of gene expression in ozone stress was significantly lower in the tolerant SL41 than in cv Nipponbare (Frei et al., 2010). From a physiological point of view, apoplastic ascorbate (AsA) has been shown to form the first line of defense against the ozone entering the plants through the stomata (Luwe et al., 1993; Plöchl et al., 2000; Feng et al., 2010), which supports the link between the annotation of the candidate gene and ozone stress tolerance. In line with this concept, a previous study demonstrated that an AO-overexpressing tobacco (*Nicotiana tabacum*) plant negatively affected tolerance to ozone due to altered apoplastic reduced AsA content and AsA redox status (Sanmartin et al., 2003). These converging pieces of evidence suggested that the expression of this putative AO gene was associated with ozone stress tolerance in rice in terms of visible symptom formation.

AO is classified as a multicopper oxidase family protein and can be found in plant and bacterial genomes (Hoegger et al., 2006). In plants, AO family proteins are localized in the apoplast, the vacuole, the tonoplast, and the Golgi apparatus (Liso et al., 2004; Balestrini et al., 2012). AO is supposedly involved in AsA metabolism in the apoplast, thereby controlling its redox status (Pignocchi and Foyer, 2003). Although several studies have been conducted on AO proteins in different plant species, its diverse roles in plant metabolism remain to be fully understood. Yamamoto et al. (2005) observed that knockdown of AO led to higher tolerance to salinity and oxidative stresses in Arabidopsis (*Arabidopsis thaliana*). Garchery et al. (2013) reported an increase in the early fruit diameter and alteration in hexose and Suc contents in leaves in AO knockdown lines in tomato (*Solanum lycopersicum*). These examples raise questions regarding the physiological role of AO genes in plants, since absence or lower expression of AO genes often appears to be favorable. In contrast, AO was also suggested to enhance cell expansion and growth (Kato and Esaka, 2000; Pignocchi et al., 2003). Due to its apparently contradictory roles, AO has been named a mysterious enzyme (Dowdle et al., 2007), of which the diverse biological functions remain to be fully elucidated.

In this study, we aimed at characterizing the previously identified putative AO gene *Os09g0365900*, which we named *OZONE-RESPONSIVE APOPLASTIC PROTEIN1* (*OsORAP1*), by specifically testing three hypotheses: (1) OsORAP1 has AO activity and is localized in the apoplast; (2) OsORAP1 affects leaf visible symptom formation in rice under chronic ozone stress; and (3) because *OsORAP1* may be the gene underlying the ozone tolerance QTL *OzT9*, it shows sequence polymorphisms between tolerant and susceptible rice cultivars.

RESULTS

Hypothesis 1: OsORAP1 Is an AO Localized in the Apoplast

The amino acid sequence of AO (EC 1.10.3.3) is highly similar to that of laccases (EC 1.10.3.2), which are also classified as multicopper oxidases and have a large number of family proteins (Hoegger et al., 2006). To analyze the phylogenetic relationship of the rice *OsORAP1* gene (*Os09g0365900*) with other similar genes, we first compared the sequence of OsORAP1 with other Arabidopsis and rice AO and laccase proteins. OsORAP1 was in the same clade as other Arabidopsis AO proteins (At5g21100, At5g21105, and At4g39830; Yamamoto et al., 2005; Fig. 1A, clade III), being closest to At4g39830 with 59% identity at the amino acid level. Three other rice proteins (Os06g0567200, Os06g0567900, and Os09g0507300) were in the same clade as the Arabidopsis AO proteins. This clade was further categorized into III-A and III-B, each including rice and Arabidopsis proteins. Analysis with other plant species also revealed clear diversification of clades III-A and III-B (Supplemental Fig. S1). All the known Arabidopsis laccase proteins were classified into clade I; therefore, we concluded that it represented the large laccase family. Another small family (clade II) was not classified as clade I or III and was termed as AO-like. The AO-like subfamily did not contain the multicopper oxidase protein domain and copper-binding site (Interpro identifier IPR002355), while all the sequences in clade III did, including OsORAP1 (Supplemental Fig. S2). The proteins in clade III also contained a protein signature L-ascorbate oxidase, plants (Interpro identifier IPR017760).

Analysis with the SignalP 4.1 program (Petersen et al., 2011) predicted a signal peptide in the first 24 amino acids and a cleavage site between amino acids 24 and 25, thereby providing evidence that OsORAP1 is a secreted protein. To experimentally confirm the subcellular localization of OsORAP1, we produced a vector construct, in which the OsORAP1 protein was fused with GFP at the C terminus, and expressed them in *Nicotiana benthamiana* leaves with the constitutive cauliflower mosaic virus (CaMV) 35S promoter. Heterologous expression in *N. benthamiana* epidermal cells showed GFP signals clearly localized in the cell periphery (Fig. 1, B–D). Signals were observed

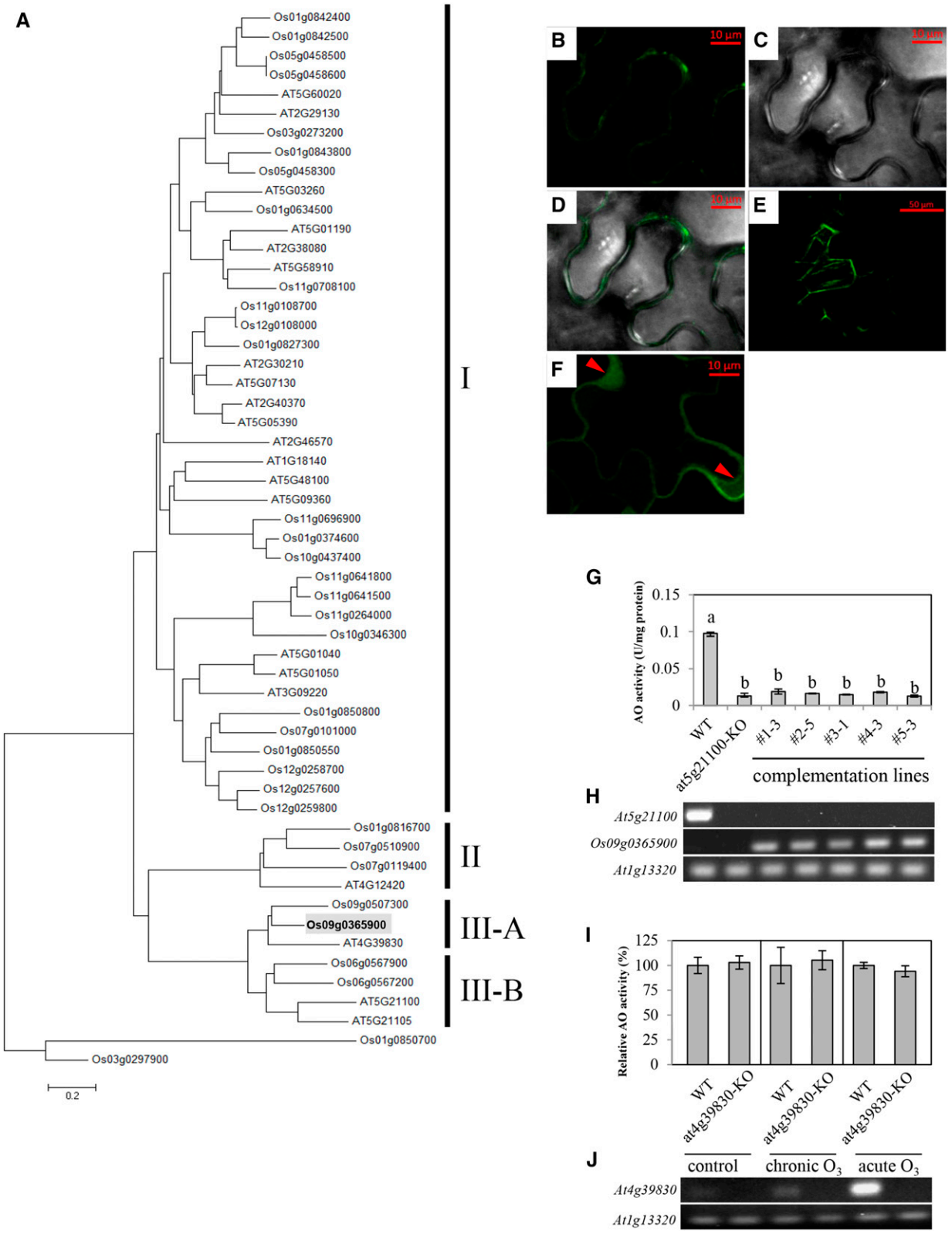

Figure 1. Bioinformatic and physiological analyses of *OsORAP1*. A, Phylogenetic analysis of laccase- and AO-related proteins from rice and Arabidopsis. The neighbor-joining method was used to generate the tree. The branch length represents the evolutionary distance calculated by the Poisson correction method. OsORAP1 (Os09g0365900) is shown in boldface and highlighted. B to F, Subcellular localization of the OsORAP1 protein in *N. benthamiana* epidermal cells (B–D and F) and mesophyll cells (E).

in the periphery of the cells in mesophyll cells as well (Fig. 1E). Upon plasmolysis (i.e. dissociation of the plasma membrane from the cell wall) in epidermal cells, the signals were observed in the apoplastic space (Fig. 1F, arrowheads), thereby confirming the apoplastic localization of OsORAP1.

Complementation analysis was conducted to examine whether OsORAP1 had AO activity. We obtained a homozygous knockout line for an Arabidopsis gene in clade III-B (*At5g21100*, SALK_108854 line) and performed an enzymatic assay of AO. Indeed, AO activity was severely reduced in this knockout line as compared with the wild type, as reported previously (Fig. 1G; Yamamoto et al., 2005). To assess whether OsORAP1 exhibits AO activity, we generated transgenic Arabidopsis plants expressing CaMV 35S::*OsORAP1* in a mutant (*At5g21100*) background. If OsORAP1 encoded a functional AO, increased AO activity would be expected in the complementation lines as compared with noncomplemented mutants. However, the decreased AO activity in the knockout line was not recovered by the introduction of *OsORAP1*, despite evidence for its constitutive expression (Fig. 1, G and H). Expression data from previous transcriptomic studies suggested that another Arabidopsis AO homolog (*At4g39830*, clade III-A) was specifically induced by ozone and biotic stresses (Supplemental Table S1). Therefore, AO activity of a homozygous knockout line of *At4g39830* (SALK_046824 line) was tested in chronic and acute ozone stress along with control conditions (Fig. 1I). *At4g39830* was strongly induced under acute ozone stress (Fig. 1J). However, AO activity level did not show marked differences between the wild type and a knockout line, despite the expression of *At4g39830* in acute ozone stress (Fig. 1, I and J), suggesting that At4g39830 did not dominate AO activity in Arabidopsis. Transient expression of native OsORAP1 protein under the regulation of the CaMV 35S promoter in *N. benthamiana* leaf also did not lead to increased AO activity, despite the expression of *OsORAP1* (Supplemental Fig. S3). Based on these observations, we confirmed that OsORAP1 was an apoplastic protein, but it had no detectable AO activity under the conditions tested in this study.

Hypothesis 2: OsORAP1 Is Involved in Ozone-Induced Cell Death in Rice

Gene Expression Analysis

To get insight into the expression patterns of *OsORAP1* in ozone stress, 4-week-old wild-type rice plants were treated either with ambient concentration of ozone (A-O_3), corresponding to the naturally occurring ozone in the greenhouse atmosphere, or with elevated ozone (E-O_3) for 20 d. First, gene expression levels were analyzed in different tissues in both conditions. Strong induction of the expression was observed only in young leaf blades ($P < 0.001$), while other tissues did not show significantly increased levels of expression (Fig. 2A). The constitutive expression level of *OsORAP1* was high in old leaves and root tissues (Fig. 2A). To investigate the function and physiological importance of OsORAP1 with respect to ozone tolerance in rice, a homozygous rice knockout line (KO) and a homozygous overexpression line (OE) were obtained (Supplemental Fig. S4A). KO did not produce any functional full-length *OsORAP1* transcript due to a transfer DNA (T-DNA) insertion (Supplemental Fig. S4B). Four-week-old plants were treated with ozone for 20 d along with the wild type. Two independent experiments were conducted, leading to similar results (see below). *OsORAP1* was highly induced by E-O_3, reaching more than 30-fold expression levels compared with A-O_3 in the wild type on day 10 (Fig. 2B). In all cases, significantly higher expression was observed in OE than in the wild type (Fig. 2B). Similar *OsORAP1* expression levels were obtained from the second ozone fumigation experiment (Supplemental Fig. S5A).

The gene expression levels of the aforementioned three putative rice AO homologs were also analyzed. The closest homolog, *Os09g0507300*, showed no expression in any of the conditions tested in our study (data not shown). The other two homologs, *Os06g0567200* and *Os06g0567900*, showed constitutive expression in the A-O_3 condition (Fig. 2, C and D). KO of *OsORAP1* showed a higher expression level of *Os06g0567200* than the other two lines ($P < 0.05$; Fig. 2C).

Figure 1. (*Continued.*)
OsORAP1 was transiently expressed under the control of the CaMV 35S promoter. The signal of GFP (B, E, and F), bright field (C), and merged images (D) are shown. In F, plasmolysis was induced by incubating the leaf segment with 1 M NaCl for 30 min prior to observation. Arrowheads indicate the dissociation of cell membrane from the cell wall and resultant signals in the apoplast. Bars = 10 μm (B–D and F) and 50 μm (E). G, AO activity of wild-type Arabidopsis plants (WT), a homozygous knockout line of *At5g21100* (at5g21100-KO), and five individual homozygous complementation lines. Values are means of four biological replicates. H, Expression of *At5g21100* (Arabidopsis AO homolog; top), *Os09g0365900* (rice *OsORAP1*; middle), and *At1g13320* (Arabidopsis reference gene; bottom). I, AO activity of the wild type and a homozygous knockout line of *At4g39830* (at4g39830-KO). The activity of the wild type was considered as 100% in each treatment, and the activity of at4g39830-KO is shown in relative values. Chronic ozone treatment was conducted at the average concentration of 110 $\pm$ 44 nL L^{-1} (7 h and 17 d), and acute ozone treatment was conducted at the average concentration of 230 $\pm$ 80 nL L^{-1} (6 h and 4 d). In all cases, rosette leaves of 4- to 6-week-old plants were used for the analysis. Values are means of four to six biological replicates. J, Expression of *At4g39830* (Arabidopsis AO homolog; top) and *At1g13320* (bottom). In G and I, error bars indicate SE.

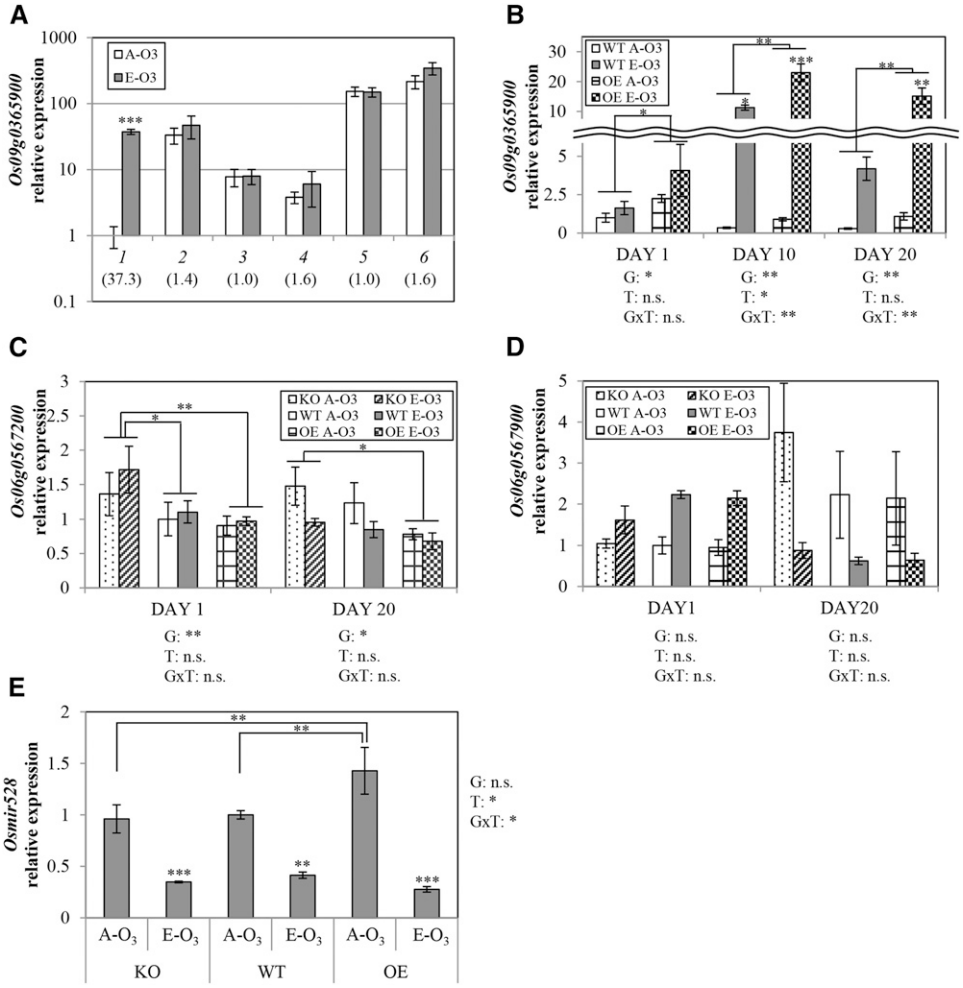

Figure 2. Expression analysis of *OsORAP1*, two other AO genes, and a microRNA, *Osmir528*. A, Expression levels of *OsORAP1* in different tissues in the A-O_3 condition (12 nL L^{-1}) and the E-O_3 condition (86 nL L^{-1}) on day 20. Different tissues used in the experiment are as follows: 1, two youngest leaf blades; 2, two oldest leaf blades; 3, outer leaf sheaths; 4, inner leaf sheaths (containing newly emerging leaves); 5, half basal part of roots; and 6, half apical part of roots. The value in the parentheses is the fold increase in the E-O_3 condition in each tissue as compared with the A-O_3 condition. Pairwise Student's *t* tests were conducted for each tissue between two treatments. Asterisks indicate a significant difference ($P < 0.001$). The *y* axis is shown in logarithmic scale. The expression level in the two youngest leaf blades in A-O_3 was determined as 1. B to E, Gene expression analysis in young shoot and leaves in the A-O_3 condition (40 nL L^{-1}) and the E-O_3 condition (159 nL L^{-1}). B, Expression levels of *OsORAP1* in A-O_3 and E-O_3 at three different time points in two different genotypes. C, Expression levels of a rice AO homolog (*Os06g0567200*) in A-O_3 and E-O_3 at two different time points in three different genotypes. D, Expression levels of a rice AO homolog (*Os06g0567900*) in A-O_3 and E-O_3 at two different time points in three different genotypes. E, Expression of the microRNA *Osmir528* on day 20. In all cases, E-O_3 treatment was started (day 1) at the 4-week-old stage. WT, The wild type. Values are means of four biological replicates (except for the wild-type A-O_3 sample on day 10, due to the loss of one sample). Error bars indicate SE. In B-E, ANOVA was conducted for each day, and the significance is denoted as follows: G, genotype; T, treatment; GxT, genotype and treatment interaction; n.s., not significant; *, $P < 0.05$; **, $P < 0.01$; and ***, $P < 0.001$.

OsORAP1 is predicted to interact with a microRNA, *Osmir528*, in rice (de Lima et al., 2012). Therefore, we analyzed the expression of *Osmir528* in all three lines (wild type, KO, and OE) in A-O_3 and E-O_3 conditions. We found that transcript abundance for *Osmir528* decreased significantly in all three lines in ozone stress (Fig. 2E; $P < 0.05$). Moreover, we also observed a significant interaction between genotype and treatment ($P < 0.05$). These observations strongly suggest that *Osmir528* is involved in the ozone-induced transcriptional regulation of *OsORAP1*.

OsORAP1 Knockout Mitigates Cell Death Formation in Ozone Stress

Growth parameters and leaf visible symptoms were measured in wild-type, KO, and OE plants to assess the effect of *OsORAP1* expression in ozone stress.

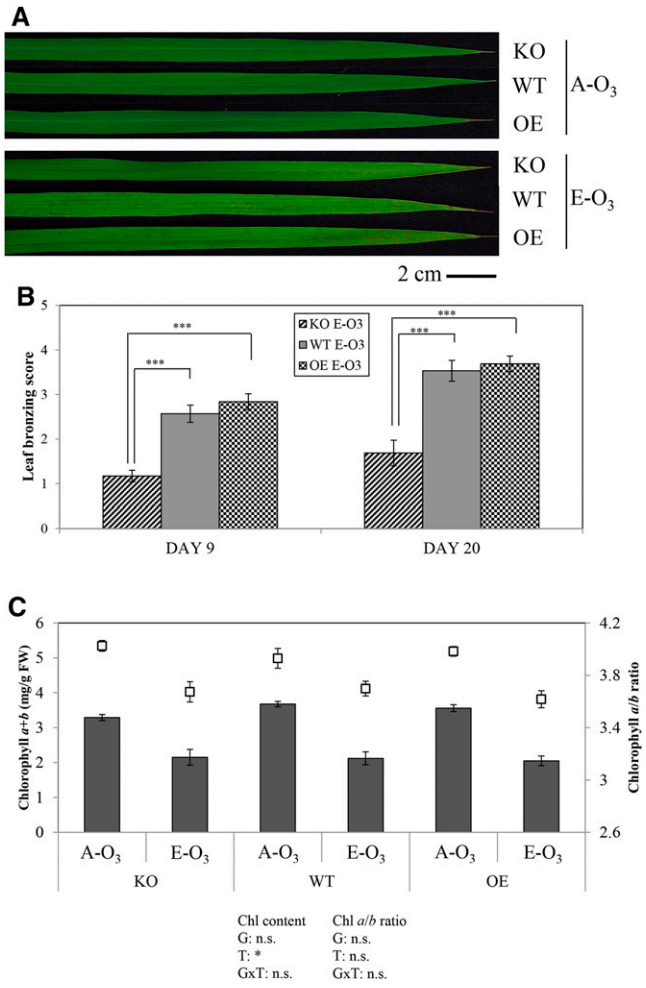

Figure 3. Formation of leaf visible symptoms and biochemical parameters in three rice lines. A, Leaf images exposed to A-O_3 (12 nL L^{-1}) or E-O_3 (86 nL L^{-1}) treatment at 15 d from the onset of the experiment. Representative second fully expanded leaves were photographed. WT, The wild type. B, LBS from three lines on days 9 and 20 in the E-O_3 condition (86 nL L^{-1}). The values are means of 20 to 22 biological replicates on day 9 and eight biological replicates on day 20. C, Chlorophyll content (bars, left axis) and chlorophyll *a*/*b* ratio (squares, right axis) in A-O_3 (40 nL L^{-1}) and E-O_3 (159 nL L^{-1}). The measurement was conducted on day 8. Elevated ozone treatment was started at the 4-week-old stage. Values are means of four biological replicates. All error bars indicate SE. FW, Fresh weight. In B and C, ANOVA was conducted, and the significance is denoted as follows: G, genotype; T, treatment; GxT, genotype and treatment interaction; n.s., not significant; *, $P < 0.05$; and ***, $P < 0.001$.

Symptoms were quantified by the leaf bronzing score (LBS; Wissuwa et al., 2006), in which a higher score indicates more damage. KO showed significantly lower LBS compared with the wild type and OE, demonstrating enhanced tolerance to ozone stress (Fig. 3, A and B). The difference in LBS was not due to differences in morphology, since the plant height, which might affect ozone uptake due to canopy resistance, was similar in all three lines (Supplemental Figs. S6 and S7A). We also did not observe significant genotypic differences in chlorophyll content or chlorophyll *a*/*b* ratio (Fig. 3C).

Stomatal conductance was measured, as ozone is mainly taken up through the stomata and the uptake is proportional to the stomatal aperture (Omasa et al., 2002). We observed a clear treatment effect ($P < 0.001$) but no significant genotype or genotype and treatment interaction effect (Fig. 4A). Growth parameters were determined on day 20. KO showed constitutively lower shoot fresh weight and tiller number compared with the wild type and OE (Fig. 4B). Significant correlation was seen between fresh weight and tiller number ($r^2 = 0.81$, $P < 10^{-7}$), suggesting that a large part of the reduced fresh weight in KO is ascribed to reduced tiller

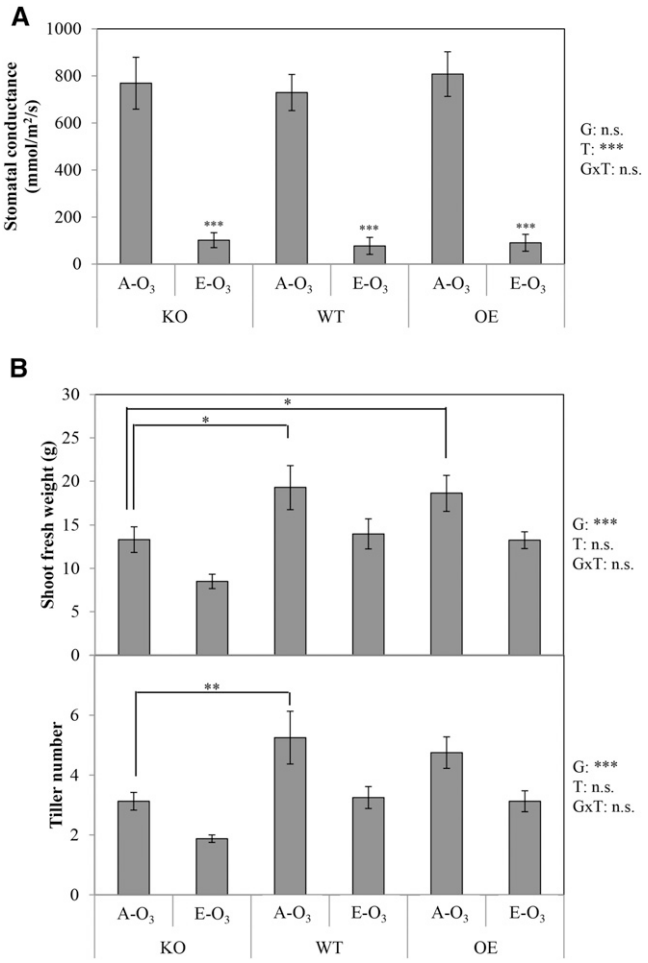

Figure 4. Effects of ozone on stomatal conductance and growth characteristics. A, Stomatal conductance of the three lines in A-O_3 (12 nL L^{-1}) and E-O_3 (86 nL L^{-1}). The measurement was conducted on day 14. The values are means of seven to 11 samples. Error bars indicate SE. B, Growth characteristics of the three lines in A-O_3 (12 nL L^{-1}) and E-O_3 (86 nL L^{-1}) on day 20. Values are means of eight biological replicates. Error bars indicate SE. E-O_3 treatment was started at the 4-week-old stage. WT, The wild type. ANOVA was conducted, and the significance is denoted as follows: G, genotype; T, treatment; GxT, genotype and treatment interaction; n.s., not significant; *, $P < 0.05$; **, $P < 0.01$; and ***, $P < 0.001$.

number. However, when grown in soil, KO showed significantly shorter flag leaf blade length, while the shape (ratio of leaf length and width) was not affected (Supplemental Fig. S7, C and D). We further investigated the leaf weight per area to estimate the cell density, since it plays an important role for ozone stress tolerance in Arabidopsis (Barth and Conklin, 2003). The analysis revealed no significant genotypic differences in the cell density among genotypes (Supplemental Fig. S8). Taken together, KO specifically mitigated foliar cell death induced by ozone stress, while other leaf properties, such as cell density and chlorophyll content, were not affected, except for leaf length.

KO Induces Less Oxidative Damage

Lipid peroxidation (assessed as malondialdehyde [MDA] equivalents) occurs even before the initiation of leaf visible symptoms and, thus, represents an indicator of oxidative stress preceding symptom formation (Ueda et al., 2013a; Höller et al., 2014b). Elevated ozone treatment increased the MDA content even on day 3 ($P < 0.01$; Fig. 5A), when the leaf symptoms had hardly emerged (data not shown). On day 3, MDA content was significantly lower in KO than in the wild type and OE. We observed a significant genotype and treatment interaction effect on day 20 ($P < 0.01$), where MDA increased significantly in the wild type and OE ($P < 0.01$), while KO did not respond significantly to ozone. We obtained similar results from the second fumigation experiment, where a significant genotype and treatment interaction effect was observed (Supplemental Fig. S5B). Next, we investigated active reactive oxygen species (ROS) production in the apoplast, since secondary ROS formation by NADPH oxidases contributes substantially to ozone damage (Overmyer et al.,

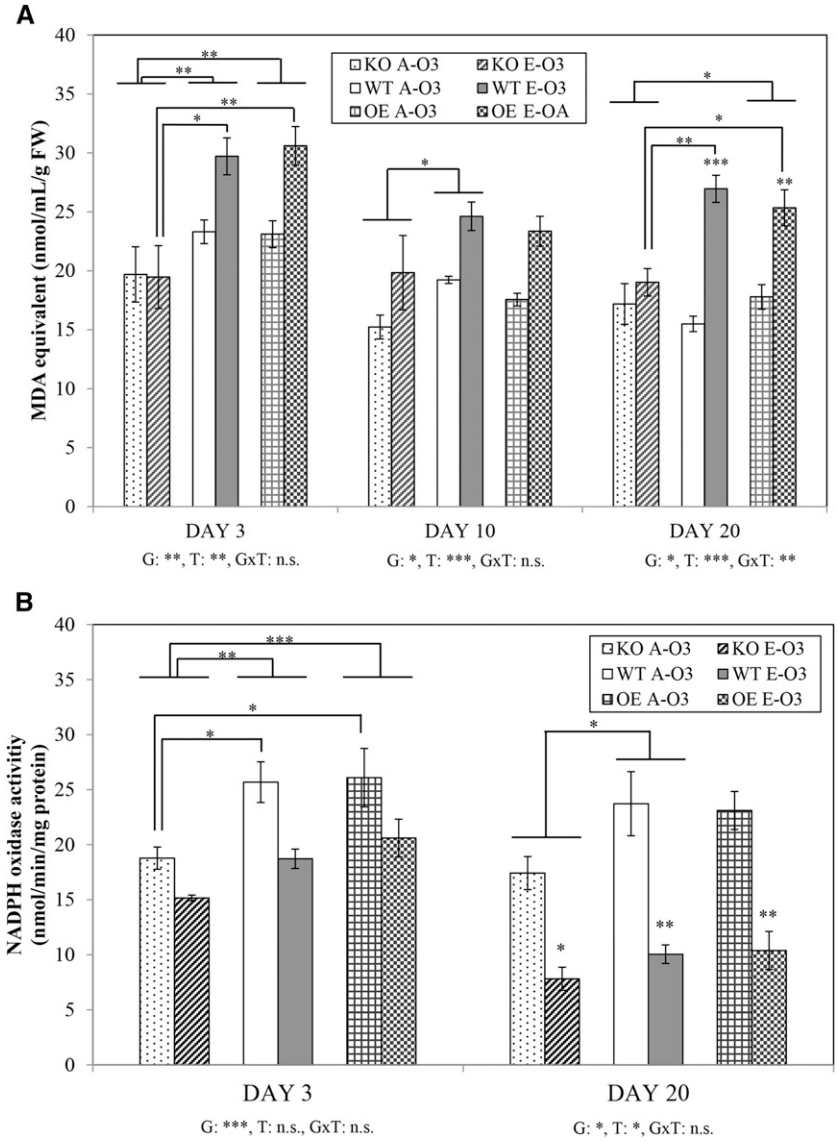

Figure 5. Measures of oxidative stress in three rice lines in A-O_3 (40 nL L^{-1}) and E-O_3 (159 nL L^{-1}). A, Lipid peroxidation as represented by MDA equivalents. FW, Fresh weight. B, NADPH oxidase activity. Elevated ozone treatment was started at the 4-week-old stage. WT, The wild type. Values are means of four biological replicates (except for the wild-type A-O_3 sample on day 10, due to the loss of one sample). Error bars indicate SE. Asterisks on E-O_3 bars show that the values were significantly affected by treatment. ANOVA was conducted, and the significance is denoted as follows: G, genotype; T, treatment; GxT, genotype and treatment interaction; n.s., not significant; *, $P < 0.05$; **, $P < 0.01$; and ***, $P < 0.001$.

2000; Wohlgemuth et al., 2002). Ozone stress significantly lowered the NADPH oxidase activity on day 20. On both days, KO showed constitutively less superoxide anion producing activity compared with the wild type (Fig. 5B).

AO Activity and Apoplastic AsA Content

As we expected based on the results obtained from the complementation assay, the knockout and overexpression of *OsORAP1*, which was classified into clade III-A (Fig. 1A), did not affect AO activity (Fig. 6A). The AO activity in the whole-tissue extract was also similar to that of the apoplastic washing fluid (Supplemental Fig. S9; $r^2 = 0.92$, $P < 0.001$), showing that the localization of the enzyme did not differ among lines or between the treatments. The expression level of one AO homolog (*Os06g0567900*, in clade III-B) showed highly significant correlation with measured AO activity (Fig. 6B), demonstrating that this homolog was the dominant AO gene in rice shoots under the conditions used for the study. Apoplastic AsA did not show any significant differences between the lines (Fig. 7), which was consistent with the lack of difference in AO activity. Likewise, AsA level or redox status in the whole shoot tissue did not show genotypic differences (Supplemental Fig. S10).

We investigated the activity of closely related laccase and other polyphenol oxidases that are also classified as copper-containing enzymes, namely catechol oxidase and Tyr oxidase (McGuirl and Dooley, 1999). However, different polyphenol oxidase activities, including laccase activity, also did not show genotypic differences (Supplemental Fig. S11).

Involvement of Plant Hormones

We investigated the involvement of plant hormones related to the formation and propagation of leaf visible symptoms in ozone stress (Rao and Davis, 2001; Kangasjärvi et al., 2005), such as ethylene, salicylic acid (SA), and jasmonic acid (JA). Through an analysis of public microarray data, it was found that *OsORAP1* is induced by exogenous SA application, which was also experimentally confirmed (Fig. 8A). To further investigate the interaction of *OsORAP1* with SA, we investigated in public microarray data sources the expression levels of *OsORAP1* in mutant lines for the transcription factor OsWRKY45, which is a regulator of SA response in rice (Shimono et al., 2007). In the first data set (National Center for Biotechnology Information [NCBI] Gene Expression Omnibus [GEO] identifier GSE23733), *OsORAP1* was induced by benzothiadiazole (a functional analog of SA), and the expression was significantly lower in a knockdown line of *OsWRKY45* compared with the wild type (Fig. 8B). Consistently, the expression of *OsORAP1* was significantly higher in the *OsWRKY45* overexpression line in the second data set (NCBI GEO identifier GSE48202; Fig. 8C).

We further analyzed the expression levels of genes that are involved in either biosynthetic or signaling pathways of the above-mentioned hormones on days 1 and 20 in our mutant lines (Fig. 8, D–H, Supplemental Fig. S12). The expression of *OsWRKY45* was higher in KO and OE than in the wild type on both days (Fig. 8D). On the other hand, the expression level of *Nonexpressor of Pathogenesis-Related Genes1* (*OsNPR1*), another transcription factor controlling the SA response (Shimono et al., 2007), was lower in KO than in the wild type on day 1 (Fig. 8E). Differential regulation of genes was also observed in JA-related genes. The enzyme 12-oxophytodienoate reductase7 (OsOPR7) is involved in JA biosynthesis in rice, and its expression level correlates with JA level (Tani et al., 2008). OsJAZ8 is involved in JA signaling, and its expression level is induced by JA application (Yamada et al., 2012). OsJAmyb is a transcription factor that is induced by JA (Lee et al., 2001). On day 20, *OsOPR7* showed significantly higher expression in KO (Fig. 8F), and the expression of *OsJAZ8* and *OsJAmyb* was significantly high on day 1 in KO (Fig. 8, G and H). The expression level of *OsJAmyb* was higher in KO even in the A-O_3 condition on day 1 (Fig. 8H).

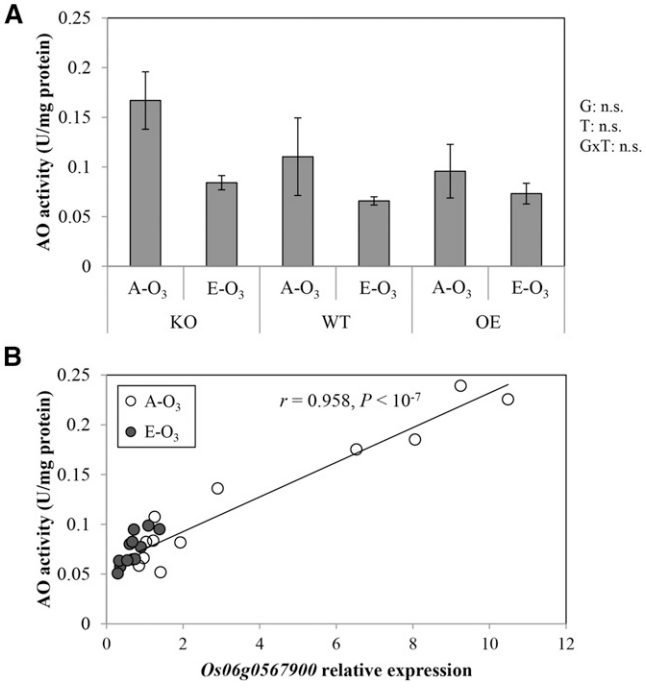

Figure 6. AO activity in A-O_3 (40 nL L^{-1}) and E-O_3 (159 nL L^{-1}). A, AO activity in the three lines. The samples were taken on day 20 of E-O_3 treatment. WT, The wild type. Values are means of four biological replicates. Error bars indicate SE. ANOVA was conducted, and the result is shown as follows: G, genotype; T, treatment; GxT, genotype and treatment interaction; and n.s., not significant. B, Correlation between the expression level of an AO homolog (*Os06g0567900*) and AO activity on day 20 in A-O_3 and E-O_3 conditions. Pearson's correlation coefficient and the corresponding *P* value are shown. Elevated ozone treatment was started at the 4-week-old stage.

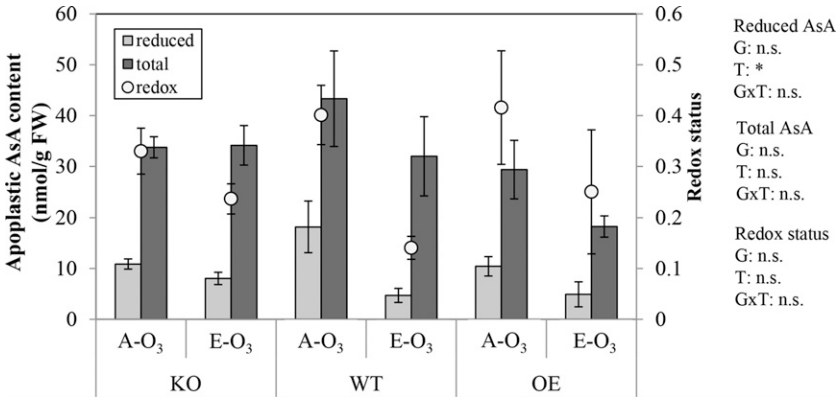

Figure 7. Apoplastic AsA characteristics in A-O_3 (12 nL L^{-1}) and E-O_3 (86 nL L^{-1}). Samples were taken at 15 d from the onset of E-O_3 treatment. Redox status was defined as (reduced AsA)/(total AsA). Elevated ozone treatment was started at the 4-week-old stage. FW, Fresh weight; WT, the wild type. Values are means of four biological replicates. Error bars indicate SE. ANOVA was conducted, and the result is shown as follows: G, genotype; T, treatment; GxT, genotype and treatment interaction; n.s., not significant; and *, $P < 0.05$.

Hypothesis 3: Sequence Variation at the OsORAP1 Locus Explains the Effect of the QTL *OzT9*

Since *OsORAP1* had been proposed as a candidate gene underlying the ozone tolerance QTL *OzT9*, we compared the genomic sequences of *OsORAP1* in the ozone-susceptible cv Nipponbare and the tolerant *OzT9* donor variety cv Kasalath (Frei et al., 2008). Our analysis revealed a number of polymorphic sites between the two cultivars in the upstream promoter region, while the coding sequence was largely conserved (Fig. 9; Supplemental Fig. S13). The deduced amino acid sequence revealed slight modifications in the signal peptide and three amino acid substitutions in the rest of the sequence (Supplemental Fig. S14). These polymorphic amino acid positions were not located at conserved amino acids, and the copper-binding sites were conserved in both cultivars. The first 30 amino acids in cv Kasalath were also predicted to be transit peptides (by SignalP 4.1); therefore, the amino acid polymorphisms in the signal peptides probably did not affect the localization of the protein. The amino acid sequence of OsORAP1 in cv Dongjin, which was the background cultivar for the mutant lines in this study, was identical to that of cv Nipponbare (Supplemental Fig. S14). We searched possible regulatory sequences in the promoter region (upstream 1,000 bp) of both cv Nipponbare and cv Kasalath to get insight into the differential expression patterns of *OsORAP1* in these two cultivars (Supplemental Tables S2–S4). In both cultivars, a W-box sequence (TTGAC) was found, which is crucial for WRKY transcription factors to bind and activate the transcription of downstream genes (Yu et al., 2001). The cv Nipponbare-specific cis-elements contained ethylene-responsive elements, A(A/T)TTCAAA (Itzhaki et al., 1994), GCCGCC (Hao et al., 1998), and AGCCGCC (Sato et al., 1996; Kitajima et al., 1998), which are supposedly binding sites of ethylene-responsive element-binding proteins.

We also analyzed the *OsORAP1* sequences in a previously reported ozone-tolerant chromosome segment substitution line, SL41, which was genetically identical to cv Nipponbare except for a 13-Mb introgression including the *OzT9* region and another introgression on chromosome 6 from the tolerant cv Kasalath (Frei et al., 2010). Our analysis showed that the sequence of SL41 at the *OsORAP1* locus was identical to that of cv Kasalath (Supplemental Fig. S13).

DISCUSSION

Cell death due to ozone stress leads to losses of photosynthetically active leaf area, which is suggested to be one of the factors limiting the total productivity of plants (Fiscus et al., 2005). Therefore, identification of the genetic factors underlying the formation of visible symptoms would potentially have a large effect on crop production in the future. Although no or only weak correlations between symptom formation and yield were seen when rice cultivars with very heterogeneous genetic backgrounds were tested (Sawada and Kohno, 2009; Ueda et al., 2015), the implications for yield became more apparent when genetically similar lines differing in symptom formation were compared (Frei et al., 2012; Wang et al., 2014). In this study, we characterized *OsORAP1*, which emerged as a candidate gene for ozone stress tolerance (i.e. the formation of cell death) in a previous study (Frei et al., 2010). To elucidate the physiological function of OsORAP1 in ozone stress, three hypotheses were tested.

Hypothesis 1: OsORAP1 Is an AO Localized in the Apoplast

Apoplastic AsA has been considered important in the context of ozone stress tolerance, as it detoxifies incoming ozone (Luwe et al., 1993; Turcsányi et al., 2000). In support of this hypothesis, altered apoplastic AsA status through the introduction of an AO gene led to differential ozone stress tolerance in tobacco plants (Sanmartin et al., 2003). In agreement with the current rice gene annotation for *OsORAP1* (L-ascorbate oxidase precursor in RAP-DB [http://rapdb.dna.affrc.go.jp/index.html] as of January 2015), phylogenetic analysis indeed showed close relatedness of OsORAP1 to Arabidopsis AO proteins. Observation of the OsORAP1-GFP fusion protein (Fig. 1, B–F) indeed determined the

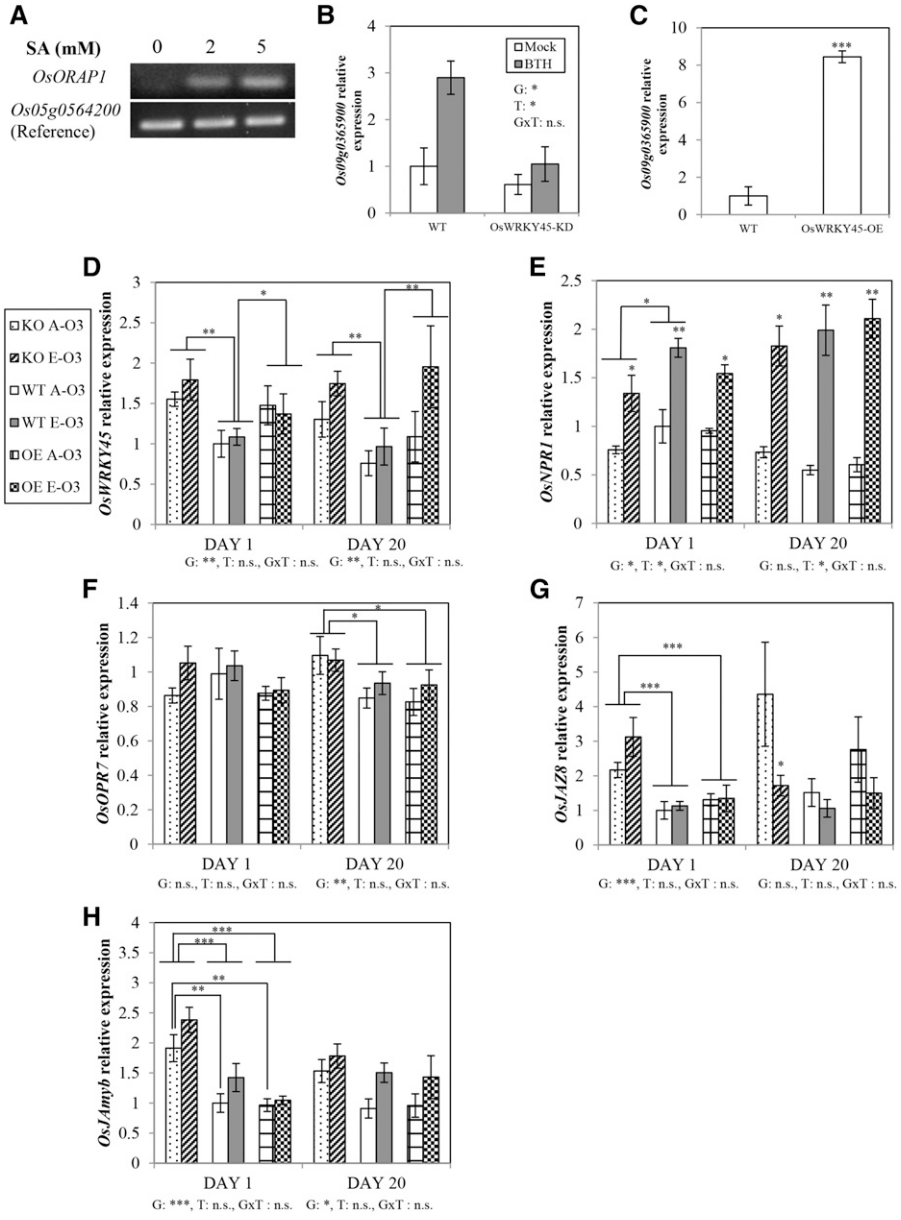

Figure 8. Involvement of OsORAP1 in phytohormone signaling. A, Induction of *OsORAP1* by SA treatment. Six-week-old plants were sprayed with the indicated concentrations of SA in 0.1% (v/v) Tween 20, and the two youngest leaves were harvested after 48 h. The expression levels of *OsORAP1* (using primers OsORAP1-F2/R2) and an internal control (*Os05g0564200*) are shown. B, Expression levels of *OsORAP1* in the wild type (WT) and an *OsWRKY45* knockdown line (OsWRKY45-KD) after mock treatment (0.05% [v/v] acetone and 0.05% [v/v] Tween 20) or benzothiadiazole (BTH) treatment (0.5 mM benzothiadiazole in 0.5% [v/v] acetone and 0.05% [v/v] Tween 20). The samples were taken after 12 h of treatment. The data were retrieved from an open microarray data source (NCBI GEO identifier GSE 23733). Original $\log_2$-converted values were processed and expressed as linear values. The expression level of the wild-type sample with mock treatment was set to 1. C, Expression levels of *OsORAP1* in the wild type and an *OsWRKY45* overexpression line (OsWRKY45-OE). The data were retrieved from an open microarray data source (NCBI GEO identifier GSE48202). Original $\log_2$-converted values were processed and expressed as linear values. The expression level of the wild-type sample was set to 1. Student's *t* test was conducted, and the asterisks indicate a significant difference ($P < 0.001$). D to H, Expression levels of phytohormone-related genes in A-O_3 (40 nL L^{-1}) and E-O_3 (159 nL L^{-1}). The gene identifiers are as follows. *OsWRKY45*, *Os05g0322900*; *OsNPR1*, *Os01g0194300*; *OsOPR7*, *Os08g0459600*; *OsJAZ8*, *Os09g0439200*; and *OsJAmyb*, *Os11g0684000*. Elevated ozone treatment was started at the 4-week-old stage. Values are means of four biological replicates. Error bars indicate SE. In B and D to H, ANOVA was conducted, and the significance is denoted as follows: G, genotype; T, treatment; GxT, genotype and treatment interaction; n.s., not significant; *, $P < 0.05$; **, $P < 0.01$; and ***, $P < 0.001$.

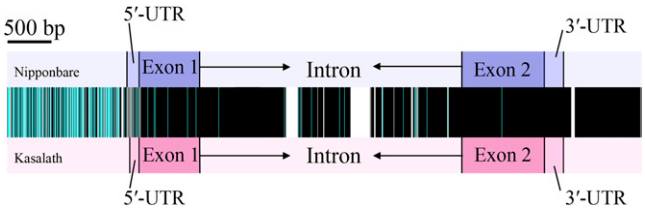

Figure 9. Sequence comparison of *OsORAP1* of cv Nipponbare (top) and cv Kasalath (bottom) rice. First, multiple alignment was conducted using MEGA5 software. Matched nucleotides are shown in black, mismatched nucleotides are shown in light blue, and gaps are shown in white. Upstream 1,500-bp, *OsORAP1* region, and downstream 1,000-bp sequences are shown. The 5′- and 3′-untranslated regions (UTR), exons, and intron are also shown for each cultivar. Bar = 500 bp.

apoplastic localization of OsORAP1, which is in accordance with bioinformatic analysis (i.e. the existence of signal peptide) and the expected localization of AO family proteins (Liso et al., 2004; Balestrini et al., 2012).

Next, we tested whether the protein had AO activity. Arabidopsis At5g21100 (clade III-B) is an AO homolog in which AO activity was previously confirmed (Yamamoto et al., 2005). Supporting these previous results, a drastic decline of AO activity was observed in a knockout line of *At5g21100* (Fig. 1G). This clearly showed that At5g21100 is responsible for a large part of the AO activity in Arabidopsis. In consequence, the lack of increased AO activity in the complemented lines (Fig. 1G) demonstrated the absence of AO activity in OsORAP1. In rice, the AO homolog Os06g0567900 dominated the AO activity in shoots (Fig. 6B). Interestingly, the dominant At5g21100 and Os06g0567900 were in the same clade III-B, while OsORAP1 and At4g39830, of which homozygous knockout lines did not show decreased AO activity, were in clade III-A (Fig. 1A; Supplemental Fig. S1). Previous transcriptomic studies and our own experiment showed that both *OsORAP1* and *At4g39830* (in clade III-A) were specifically induced under oxidative and biotic stresses, while *Os06g0567900* and *At5g21100* (in clade III-B) were suppressed or less affected by these treatments, with the exception of methyl viologen (MV) treatment (Supplemental Tables S1 and S5). These data suggest that different subclades might represent different molecular functions. Taken together, the apoplastic localization, but not the AO activity, of OsORAP1 was confirmed in this study.

A constitutively high expression level of *OsORAP1* was observed in root tissues, especially in the half apical side of the root (Fig. 2A). According to a previous microarray study (Sato et al., 2011), high expression was observed in the root cap (Supplemental Fig. S15). Moreover, our further investigations into the possible molecular functions revealed that *OsORAP1* was highly induced during seed imbibition (Supplemental Fig. S16). Supporting this, a homozygous knockout line of *OsORAP1* (identifier M0083940-8-A) in the genetic background of cv Tainung 67 (a *japonica* rice cultivar) was lethal (Supplemental Table S6). Therefore, OsORAP1 might be related to embryogenesis or cell elongation. It also seems that OsORAP1 is involved in leaf expansion and tiller formation (Fig. 4; Supplemental Fig. S7). This observation is similar to previous findings that AO family proteins enhanced cell elongation and growth rate in tobacco (Kato and Esaka, 2000; Pignocchi et al., 2003). The molecular function of OsORAP1 warrants further detailed investigations.

Hypothesis 2: OsORAP1 Is Involved in Ozone-Induced Cell Death in Rice

KO was more tolerant to ozone stress in terms of leaf visible symptom formation and lipid peroxidation (Figs. 3, A and B, and 5A), and the lower superoxide anion production rate further supported that KO experienced less oxidative damage (Fig. 5B). The AO activity and apoplastic AsA content did not show any significant differences between the lines (Figs. 6A and 7), implying that tolerance in KO was not the consequence of higher ozone-detoxifying capacity through AsA in the apoplast. Apart from apoplastic AsA, mutant screening experiments in Arabidopsis have revealed several tolerance mechanisms to ozone stress to date. These include AsA content, stomatal conductance, and leaf parenchyma cell density (Conklin et al., 1996; Barth and Conklin, 2003; Overmyer et al., 2008; Vahisalu et al., 2008). In this study, none of these traits were significantly affected in *OsORAP1* mutant lines compared with the wild type (Fig. 4A; Supplemental Figs. S8 and S10), indicating that KO shows tolerance due to a novel mechanism. Chlorophyll content, which decreases during senescence (Miller et al., 1999), thus reflecting the overall stress levels of leaves, also did not show any genotypic differences (Fig. 3C). Together, these data suggest that KO of *OsORAP1* specifically mitigated cell death by a novel mechanism, but not antioxidant capacity or the general status of leaves as affected by ozone.

Induction of *OsORAP1* in ozone stress was specific to young leaf blades, which had very low expression in the A-O_3 condition (Fig. 2B). In other words, gene expression was induced in photosynthetically active tissues with high intake of ozone, since older rice leaves have reduced stomatal aperture resulting in reduced ozone influx (Maggs and Ashmore, 1998). Besides ozone stress, *OsORAP1* was also induced by pathogen infection and MV stress (Supplemental Table S5). Both ozone and pathogen infections induce apoplastic oxidative stress and, consequently, programmed cell death (PCD) if ROS formation exceeds a certain threshold (Heath, 2000; Kangasjärvi et al., 2005). Cell death under MV stress also shares similar characteristics with PCD (Chen and Dickman, 2004; Chen et al., 2009). In addition, PCD plays an important role during embryogenesis (Helmersson et al., 2008) and in the

root cap (Pennell and Lamb, 1997), where *OsORAP1* is highly expressed (Supplemental Figs. S15 and S16). These facts imply that *OsORAP1* is closely related to PCD, possibly via ROS, while it is not induced under many other abiotic stresses, such as zinc deficiency (Supplemental Table S5), where the foliar symptoms are assumed to occur via traumatic oxidative damage, not via PCD (Cakmak, 2000).

SA was another factor inducing *OsORAP1*, although SA itself does not induce PCD. This induction could occur either due to SA itself or apoplastic ROS accumulation caused by SA application (Kawano and Muto, 2000; Khokon et al., 2011). The expression pattern of *OsORAP1* in *OsWRKY45* mutant lines strongly suggested that its expression is highly OsWRKY45 dependent. The presence of a W-box (Eulgem et al., 2000) in the promoter region of *OsORAP1* supports this concept. Although no induction of *OsWRKY45* was observed in our study, OsWRKY45 might be post-translationally processed and affect the expression level of downstream genes (Matsushita et al., 2013). Gene expression levels of JA-related genes (*OsOPR7*, *OsJAZ8*, and *OsJAmyb*) suggested that JA production is enhanced in KO. Higher expression of *OsWRKY45* in KO might be due to the fact that it is also induced by JA as well as SA (De Vleesschauwer et al., 2013). JA counteracts ROS production and the effect of SA and ethylene, which promote cell death, thus containing the spread of cell death caused by ozone (Overmyer et al., 2000, 2003; Kangasjärvi et al., 2005). Therefore, the mitigation of cell death in KO is probably associated with the JA signaling pathway.

Hypothesis 3: Sequence Variation at the OsORAP1 Locus Explains the Effect of the QTL *OzT9*

The sequence analysis of different rice cultivars revealed highly conserved amino acid sequences and highly divergent promoter regions (Fig. 9; Supplemental Fig. S13). The lower *OsORAP1* expression in ozone stress in the tolerant line SL41 as compared with cv Nipponbare (Frei et al., 2010) might be explained by cis-elements such as ethylene-responsive element-binding sites specific to the cv Nipponbare promoter sequence. Moreover, retarded growth during the vegetative growth stage seen in KO was also observed in SL41 in a previous study (Frei et al., 2008), further supporting the possibility that *OsORAP1* is the causative gene underlying the effect of *OzT9*. However, we did not observe differences in AsA content of the whole tissue and apoplast between the lines, as seen previously between cv Nipponbare and SL41 (Fig. 7; Supplemental Fig. S10; Frei et al., 2010), suggesting that other genes might add to the effect of *OzT9* in SL41. Nucleotide polymorphisms in the promoter or regulatory sequence of a gene have been suggested to underlie several QTLs in rice, such as blast resistance (Davidson et al., 2010) and flowering time (Kojima et al., 2002; Takahashi et al., 2009). Similarly, in this study, the expression level of *OsORAP1*, rather than functional alteration, could be the causal polymorphism for *OzT9*. Fine-mapping of *OzT9*, further transgenic approaches (e.g. swapping the gene and promoter of *OsORAP1* between contrasting cultivars), and analysis of naturally occurring polymorphisms in the *OsORAP1* promoter region and their correlation with ozone tolerance are warranted to confirm this conclusion.

CONCLUSION AND OUTLOOK

Regarding the hypotheses tested in this study, it can be concluded that (1) OsORAP1 is an apoplastic protein similar to an AO, but it has no measurable AO activity, (2) OsORAP1 enhances leaf visible symptoms and lipid peroxidation in ozone stress and interacts with plant hormones, and (3) sequence polymorphisms in the promoter region of *OsORAP1* supported the idea that it may underlie the effect of the QTL *OzT9*. Based on the results obtained in this study, we hypothesize that OsORAP1 is an apoplastic protein acting as a hub for signal transduction in ozone stress in rice (Fig. 10). As a future perspective, the molecular function of OsORAP1 needs to be further elucidated. Considering the localization of OsORAP1, a metabolomics analysis of apoplastic fluid (Floerl et al., 2012) would presumably be helpful in identifying its substrate (Fridman and Pichersky, 2005; Pourcel et al., 2005). It is also quite tempting to examine the pathogen resistance of the lines used in the study. This has implications beyond the breeding of ozone resistance, because PCD plays an important role in pathogen resistance by confining pathogens in dead cells, thereby preventing their spread to the other tissues (Apel and Hirt, 2004). OsORAP1 may be representative of the conflicting roles of intentional PCD due to pathogen attack and unintentional PCD due to ozone influx and, therefore, warrants further investigation.

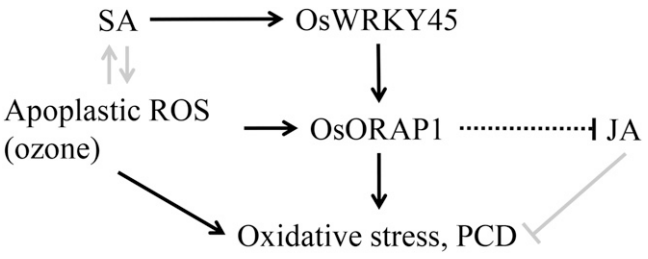

Figure 10. Hypothetical mode of action of OsORAP1 in rice. Apoplastic ROS (ozone) leads to oxidative stress and, consequently, PCD, directly or via OsORAP1. SA induces *OsWRKY45* expression (Shimono et al., 2007), and OsWRKY45 induces OsORAP1. OsORAP1 might possibly interact with the JA pathway (shown with the dotted line). The enhanced production of SA by ROS, production of ROS by SA, and preventive role of JA in cell death in ozone stress are established in other plant species (Rao et al., 2000, 2002; Khokon et al., 2011) but not yet in rice; therefore, these are shown with gray lines.

MATERIALS AND METHODS

Sequence Analysis

Rice (*Oryza sativa*) putative AO and laccase amino acid sequences were obtained from the RAP-DB Web site (http://rapdb.dna.affrc.go.jp/, as of December 2013; Sakai et al., 2013). Putative Arabidopsis (*Arabidopsis thaliana*) AO and laccase amino acid sequences were obtained from the National Center for Biotechnology Information database (http://www.ncbi.nlm.nih.gov/, as of December 2013). MEGA5 software (Tamura et al., 2011) was used to create a phylogenetic tree using the neighbor-joining method (Saitou and Nei, 1987). Protein motifs were searched through the Interpro database (http://www.ebi.ac.uk/interpro/, as of December 2013).

Construction of Vectors and Plant Transformation

The vectors for transformation were constructed using the Gateway cloning system (Curtis and Grossniklaus, 2003) as detailed in Supplemental Protocol S1. Transient expression was conducted using *Nicotiana benthamiana* leaves. These were infiltrated with *Agrobacterium tumefaciens* strain GV3101 carrying the vector pMDC83-OsORAP1 together with *A. tumefaciens* carrying pBIN61-P19 (a gift of Dr. H. Bohlmann). P19 is an RNA-silencing inhibitor, which enhances the expression of transgenes (Shah et al., 2013). Each bacterium was infiltrated at an optical density at 600 nm = 2 in a buffer consisting of 10 mM MES (pH 5.6), 10 mM $MgCl_2$, and 100 μM acetosyringone, and the signal was observed after 5 d using the LSM 710 confocal microscope (Carl Zeiss). The wavelength was 488 nm for excitation and 514 to 550 nm for emission. Plasmolysis was induced by incubating the leaf segment with 1 M NaCl (Libault et al., 2010) for 30 min. Mesophyll cells were directly observed by removing the epidermal cell layer using a razor blade and tweezers from the abaxial side.

Stable transformation of Arabidopsis was conducted by the floral dip method (Clough and Bent, 1998). Young flowers and buds of Arabidopsis plants (a homozygous knockout line: SALK_108854 for *At5g21100*, background ecotype Columbia-0) were dipped into *A. tumefaciens* (carrying pMDC32-OsORAP1 vector) solution (optical density at 600 nm = 0.8) contained in 5% (w/v) Suc solution added with 0.05% (v/v) Silwet L-77. Selection of transformants was conducted on one-half-strength Murashige and Skoog medium containing 50 μg mL^{-1} hygromycin. Homozygous T3 seeds were used for the experiments.

Plant Material and Stress Treatment

T1 seeds of two rice T-DNA insertion lines, 4A-00477 and 1B-00611, were obtained from the Crop Biotech Institute at Kyung Hee University (Jeon et al., 2000; Jeong et al., 2006). These T-DNA lines had been transformed using the *japonica* cv Dongjin as the wild type and the transformation vector pGA2715, which transfers an 8.3-kb T-DNA insertion containing four tandem sequence repeats of a transcriptional enhancer element from the CaMV 35S promoter. Line 4A-00477 (OE) contained the T-DNA insertion in 462 bp upstream of *OsORAP1*, while line 1B-00611 (KO) contained the insertion in the intron of *OsORAP1* (Supplemental Fig. S4A). The presence of the insertion near the gene should lead to overexpression via activation tagging, while an insertion in the intron should lead to suppressed expression (Jeong et al., 2002). The presence and orientation of the insertion were confirmed by PCR using genomic DNA as a template and the T-DNA right border primer 5′-AACGCTGATCAATTC-CACAG-3′ in combination with one of the following gene-specific primers: 5′-TGCAGGTTTCGTTGTCTCTG-3′ (left) or 5′-GGACGCGGTGCTATCTT-TAC-3′ (right) for line 4A-00477 and 5′-TCGCACCAATATCGAGACAG-3′ (left) and 5′-AGCGAGATGCATGTCAACTG-3′ (right) for line 1B-00611. Homozygous plants were selected in the T2 generation and used for the experiments. The seeds were sterilized with 5% (w/v) sodium hypochlorite solution for 5 min and rinsed five times with deionized water before imbibition. The seeds were germinated at 28°C in the dark, and the seedlings were then transferred to a mesh floating on deionized water placed under natural light in a greenhouse. After growing for 2 weeks, the seedlings were transplanted into 60-L plastic containers filled with one-half-strength Yoshida solution (Yoshida et al., 1976). One container accommodated a total of 40 plants of the three lines (KO, OE, and wild type) in a random distribution. The solution was changed to full strength 3 d before the onset of ozone fumigation, and the solution was renewed every 10 d. Supplementary lighting was provided in the greenhouse from 7 AM until 8 PM every day to ensure a minimum photosynthetic photon flux density of 250 μmol s^{-1} m^{-2}. The minimum temperature of the greenhouse was set to 30°C/25°C (day/night). The temperature was controlled by an inner heating system and ventilation through opening roofs. Therefore, plants were exposed to ambient ozone concentration. Arabidopsis was grown in a closed greenhouse, and the ozone concentration in the greenhouse was close to zero.

Ozone fumigation was conducted in open-top chambers (1.3-m width × 1-m length × 1.3-m height) surrounded by transparent plastic sheets. Ozone was generated using custom-made ozone generators (UB01; Gemke Technik) after drying the air with silica gel. The generated ozone was first percolated through water to remove nitrogen oxides and then blown into perforated plastic tubes with a fan to achieve an even distribution of ozone in the chambers. The ozone concentration was permanently monitored by ozone sensors (GE 703 O3; Dr. A. Kuntze) for real-time regulation of the generators. In addition, the ozone concentration was independently monitored with a hand-held ozone monitor (series 500; Aeroqual) placed within the canopy. Two independent chambers were used for E-O_3 treatment, and control plants exposed to A-O_3 were placed in identical chambers without ozone fumigation to ensure the same microclimate in both treatments. Each chamber contained two of the hydroponic containers described above.

Experiment 1

This experiment was conducted from June to August 2012. The target ozone concentration was set to 150 nL L^{-1} because of relatively high A-O_3 in the experimental area. The actually recorded average daytime ozone concentration of the E-O_3 treatment was 159 ± 64 nL L^{-1} (average ± SD, same below; 9 AM to 4 PM), while the average concentration of A-O_3 chambers was 40 ± 14 nL L^{-1}. Gene expression analysis except for tissue-specific expression, biochemical analyses except for apoplastic AsA, and AO and NADPH oxidase activity analyses were conducted in this experiment. Plant materials were harvested on the indicated days, flash frozen in liquid nitrogen, and stored at −80°C until analysis. Young shoots and leaves (top half of the shoot) were used for the analyses. The plants were 7 weeks old (counting from germination) after 20 d of fumigation.

Experiment 2

This experiment was conducted from July to October 2014. The target concentration was set to 90 nL L^{-1}. The actually measured average concentration of the E-O_3 treatment was 86 ± 32 nL L^{-1} (9 AM to 4 PM), while that of A-O_3 chambers was 12 ± 8 nL L^{-1}. Visible symptoms on the leaves were determined as LBS. The four youngest fully expanded leaves of each plant were assigned an LBS ranging from 0 (completely healthy) to 10 (dead) and averaged for each plant. Growth parameters, LBS, apoplastic AsA, stomatal conductance, tissue-specific expression levels of *OsORAP1*, and polyphenol oxidase activity were measured in this experiment (Supplemental Protocol S2). Stomatal conductance was measured using a LI-1600 Steady State Porometer (LI-COR). The measurement was conducted on day 14 on the youngest fully expanded leaves. At least nine plants were taken for the measurement from each treatment and genotype, and the highest and lowest values were excluded. The measurements were conducted within 3 h around noon on a cloudless day. The plants were 7 weeks old after 20 d of fumigation. Although different concentrations were adopted in these two experiments, the physiological responses of the plants were similar between these two experiments, as judged by the expression of *OsORAP1* and the content of lipid peroxidation (Supplemental Fig. S5), probably due to the climate conditions and the extent of ozone stress that the plants suffered before the onset of fumigation.

RNA Extraction and Gene Expression Analysis

The samples were ground in liquid nitrogen to a fine powder, and RNA was extracted with a PeqGOLD Plant RNA extraction kit (Peqlab) according to the manufacturer's protocol, including DNase digestion using RQ1 DNase (Promega). The extracted RNA was precipitated with ethanol for further purification, and the pellet was dissolved in TE buffer (10 mM Tris-HCl and 1 mM EDTA, pH 8.0). The RNA concentration was measured with a Nanodrop 2000C instrument (Thermo Fisher Scientific), and the integrity was checked using a 2100 Bioanalyzer (Agilent Technologies). Reverse transcription was performed with a GoScript Reverse Transcription System (Promega) using both oligo(dT) primers and random hexamer primers according to the manufacturer's protocol using 300 ng of RNA (except for microRNA analysis).

MicroRNA was quantified according to Lima et al. (2011). Total RNA was reverse transcribed using M-MLV Reverse Tramscriptase (Promega). The reaction mixture contained 500 ng of total RNA, 6 μL of 5× reaction buffer, 1.5 μL of 1 μM stem-loop primer (5′-GTCGTATCCAGTGCAGGGTCCGAGGTATT-CGCACTGGATACGCANNNNNN-3′), 1 μL of 10 mM deoxyribonucleotide

triphosphate mix, 25 units of RNase inhibitor, and 0.5 μL of reverse transcriptase in a 30-μL scale. The reaction was performed using the following conditions: 30 min at 16°C, 30 min at 42°C, and 5 min at 85°C.

Quantitative PCR was performed with the StepOnePlus real-time PCR system (Applied Biosystems). The reaction mixture consisted of 5 μL of GoTaq qPCR Master Mix (Promega), 0.2 μL of each gene-specific primer (10 μM; Supplemental Table S7), 3.6 μL of nuclease-free water, and 1 μL of complementary DNA sample. The reaction mixture was denatured at 95°C for 10 min, followed by 40 cycles of 15 s of denaturation at 95°C, and 1 min of annealing and extension at 60°C. Melting curves were analyzed after each reaction to check primer specificity. A housekeeping gene, *Os05g0564200*, was used as an internal control (Höller et al., 2014a). The quantification of target genes was performed using the comparative threshold cycle method as described by Frei et al. (2010). The efficiency of amplification was checked for all primer pairs using a complementary DNA dilution series, and the values between 80% and 112% were obtained. All gene expression analyses were conducted in analytical duplicates.

Enzyme Assays

AO Activity

AO activity was measured according to Pignocchi et al. (2003). Briefly, the enzyme was extracted with 1 mL of 0.1 M sodium phosphate buffer (pH 6.5) from around 80 mg of sample ground in liquid nitrogen. The ion concentration was high enough to extract the AO from the cell wall, since another extract using the same buffer including 1 M NaCl after the first extraction step retrieved only negligible AO activity in rice and Arabidopsis. The assay mixture consisted of 10 μL of the enzyme extract, 80 μL of sodium phosphate buffer (pH 5.6), and 10 μL of 2 mM reduced AsA. The solution was mixed by pipetting, and the kinetics were read at 265 nm (extinction coefficient [ε] = 14.3 mM^{-1} cm^{-1}) with a microplate reader (Powerwave XS2; BioTek). The protein concentration was measured according to the method of Bradford (1976).

NADPH Oxidase Activity

NADPH oxidase activity was measured according to Ishibashi et al. (2010). First, the enzyme was extracted from around 60 mg of frozen sample with 1 mL of 10 mM sodium phosphate buffer (pH 6.0) and two times 15-s sonication. The supernatant was obtained by centrifugation at 16,000*g* at 4°C for 15 min. An aliquot of 200 μL of the extract was mixed with 1.8 mL of 100% (v/v) acetone and placed at −20°C for more than 15 min. The protein was recovered by centrifugation at 12,500 rpm at 4°C for 10 min. The pellet was dissolved in 50 mM Tris-HCl (pH 8.0) containing 0.1 mM $MgCl_2$, 0.25 M Suc, and 0.1% (v/v) Triton X-100. The assay mixture consisted of 10 μL of the protein extract, 10 μL of 5 mM nitroblue tetrazolium, 10 μL of 1 mM NADPH, and 70 μL of the above-mentioned Tris buffer containing $MgCl_2$, Suc, and Triton X-100. The kinetics were read at 530 nm (ε = 12.8 mM^{-1} cm^{-1}), and the activity was calculated based on the protein concentration.

Biochemical Assays

AsA Assay

Extraction and quantification of AsA from the apoplast and the whole tissue were based on Ueda et al. (2013b). The reduced AsA content was measured from the absorption decrease at 265 nm after the addition of 10 μL of 0.01 units $μL^{-1}$ AO to a mixture of 10 μL of extracted AsA and 80 μL of 0.1 M potassium phosphate buffer (pH 7.0). The oxidized AsA content was measured from the absorption increase at 265 nm after the addition of 10 μL of 4 mM dithiothreitol to a mixture of 10 μL of extracted AsA and 80 μL of 0.1 M potassium phosphate buffer (pH 7.8). The calculation of the AsA content was based on the extinction coefficient of ε = 14.3 mM^{-1} cm^{-1}.

Chlorophyll Measurements

Chlorophyll content was measured according to Porra et al. (1989) using dimethylformamide as a solvent. Approximately 10 mg of fresh sample was taken from the middle part of the second fully expanded leaf, put into a 1.5-mL tube together with 1 mL of dimethylformamide without grinding, and stored at 4°C for 24 h. The absorption of the resultant solution was read at 647, 664, and 750 nm (background) using a microplate reader. The concentrations of chlorophylls *a* and *b* were calculated by the following formulae:

$$\text{Chl } a = [12.00 \times (A_{664} - A_{750}) - 3.11 \times (A_{647} - A_{750})]/0.29$$

$$\text{Chl } b = [20.78 \times (A_{647} - A_{750}) - 4.88 \times (A_{664} - A_{750})]/0.29$$

Here, 0.29 denotes the path length (cm) of the solution when 100 μL was put onto a 96-well plate (no. 3635; Corning).

MDA Quantification

The amount of MDA was determined as described previously (Hodges et al., 1999; Höller et al., 2014b). Extraction was performed from approximately 100 mg of ground tissues with 2 mL of 0.1% (w/v) TCA. The supernatant was obtained after centrifugation at 4°C and 15,000*g* for 15 min. An aliquot of 250 μL of the supernatant was mixed with 250 μL of 20% (w/v) TCA, 0.01% (w/v) 2,6-di-*tert*-butyl-4-methylphenol, and 0.65% (w/v) thiobarbituric acid. The mixture was heated to 95°C for 30 min, and the absorbance of the supernatant was measured at 440, 532, and 600 nm. The absorption of blank samples, which did not contain thiobarbituric acid, was subtracted for each sample.

Statistical Analyses

Statistical analyses were performed using the SAS program (SAS Institute) applying a PROC MIXED model. Genotype, treatment, and genotype and treatment interaction were set as fixed effects, and chamber and chamber × container were set as random effects, as described by Frei et al. (2011). Tukey's test was conducted as a posthoc test. *P* values below 0.05 were considered to be significant.

Sequence data from this article can be found in the GenBank/EMBL data libraries under the following accession numbers: OsORAP1 genomic sequence for Dongjin (KT369010) and Kasalath (KT369009).

Supplemental Data

The following supplemental materials are available.

Supplemental Figure S1. Phylogenetic analysis of clade III from 14 different plant species.

Supplemental Figure S2. Multiple alignment of the proteins in clades II and III.

Supplemental Figure S3. Transient expression of OsORAP1 in *N. benthamiana* leaves.

Supplemental Figure S4. Gene model of *OsORAP1*.

Supplemental Figure S5. Expression of *OsORAP1* and MDA content from experiment 2.

Supplemental Figure S6. Plant shape in A-O_3 and E-O_3 conditions.

Supplemental Figure S7. Growth parameters of three lines.

Supplemental Figure S8. Leaf dry weight per area in three lines.

Supplemental Figure S9. AO activity in the apoplast.

Supplemental Figure S10. Ascorbate content and redox status of whole-tissue extract.

Supplemental Figure S11. Polyphenol oxidase activity.

Supplemental Figure S12. Expression levels of phytohormone-related genes.

Supplemental Figure S13. Sequence alignment of the *OsORAP1* locus from four different rice lines.

Supplemental Figure S14. Sequence alignment of OsORAP1 proteins from four different rice lines.

Supplemental Figure S15. Expression pattern of *OsORAP1* in rice root.

Supplemental Figure S16. Expression of *OsORAP1* during seed imbibition.

Supplemental Table S1. Expression profile of Arabidopsis AO homologs under several conditions.

Supplemental Table S2. cis-Elements found only in cv Nipponbare.

Supplemental Table S3. cis-Elements found in both cv Nipponbare and cv Kasalath.

Supplemental Table S4. cis-Elements found only in cv Kasalath.

Supplemental Table S5. Expression profile of *OsORAP1* and *Os06g0567900* under several conditions.

Supplemental Table S6. Seed germination test of an *OsORAP1* knockout line in the cv Tainung 67 genetic background.

Supplemental Table S7. Primers used for this study.

Supplemental Protocol S1. Method for vector construction.

Supplemental Protocol S2. Method for polyphenol oxidase activity measurement.

ACKNOWLEDGMENTS

We thank Dr. Holger Bohlmann (University of Natural Resources and Life Sciences, Vienna) for providing pBIN61-P19 vector, Dr. Rogerio Margis (Federal University of Rio Grande do Sul) for useful advice on microRNA analysis, and Dr. Florian M.W. Grundler and Philipp Gutbrod (University of Bonn) for sharing experimental facilities and technical support on vector construction.

Received June 22, 2015; accepted July 22, 2015; published July 28, 2015.

LITERATURE CITED

Ainsworth EA (2008) Rice production in a changing climate: a meta-analysis of responses to elevated carbon dioxide and elevated ozone concentration. Glob Change Biol **14:** 1642–1650

Ainsworth EA, Yendrek CR, Sitch S, Collins WJ, Emberson LD (2012) The effects of tropospheric ozone on net primary productivity and implications for climate change. Annu Rev Plant Biol **63:** 637–661

Apel K, Hirt H (2004) Reactive oxygen species: metabolism, oxidative stress, and signal transduction. Annu Rev Plant Biol **55:** 373–399

Balestrini R, Ott T, Güther M, Bonfante P, Udvardi MK, De Tullio MC (2012) Ascorbate oxidase: the unexpected involvement of a 'wasteful enzyme' in the symbioses with nitrogen-fixing bacteria and arbuscular mycorrhizal fungi. Plant Physiol Biochem **59:** 71–79

Barth C, Conklin PL (2003) The lower cell density of leaf parenchyma in the *Arabidopsis thaliana* mutant *lcd1-1* is associated with increased sensitivity to ozone and virulent *Pseudomonas syringae*. Plant J **35:** 206–218

Bradford MM (1976) A rapid and sensitive method for the quantitation of microgram quantities of protein utilizing the principle of protein-dye binding. Anal Biochem **72:** 248–254

Cakmak I (2000) Possible roles of zinc in protecting plant cells from damage by reactive oxygen species. New Phytol **146:** 185–205

Chen R, Sun S, Wang C, Li Y, Liang Y, An F, Li C, Dong H, Yang X, Zhang J, et al (2009) The *Arabidopsis PARAQUAT RESISTANT2* gene encodes an *S*-nitrosoglutathione reductase that is a key regulator of cell death. Cell Res **19:** 1377–1387

Chen S, Dickman MB (2004) Bcl-2 family members localize to tobacco chloroplasts and inhibit programmed cell death induced by chloroplast-targeted herbicides. J Exp Bot **55:** 2617–2623

Clough SJ, Bent AF (1998) Floral dip: a simplified method for *Agrobacterium*-mediated transformation of *Arabidopsis thaliana*. Plant J **16:** 735–743

Conklin PL, Williams EH, Last RL (1996) Environmental stress sensitivity of an ascorbic acid-deficient *Arabidopsis* mutant. Proc Natl Acad Sci USA **93:** 9970–9974

Curtis MD, Grossniklaus U (2003) A Gateway cloning vector set for high-throughput functional analysis of genes in planta. Plant Physiol **133:** 462–469

Davidson RM, Manosalva PM, Snelling J, Bruce M, Leung H, Leach JE (2010) Rice germin-like proteins: allelic diversity and relationships to early stress responses. Rice **3:** 43–55

de Lima JC, Loss-Morais G, Margis R (2012) MicroRNAs play critical roles during plant development and in response to abiotic stresses. Genet Mol Biol **35:** 1069–1077

De Vleesschauwer D, Gheysen G, Höfte M (2013) Hormone defense networking in rice: tales from a different world. Trends Plant Sci **18:** 555–565

Dowdle J, Ishikawa T, Gatzek S, Rolinski S, Smirnoff N (2007) Two genes in *Arabidopsis thaliana* encoding GDP-L-galactose phosphorylase are required for ascorbate biosynthesis and seedling viability. Plant J **52:** 673–689

Eulgem T, Rushton PJ, Robatzek S, Somssich IE (2000) The WRKY superfamily of plant transcription factors. Trends Plant Sci **5:** 199–206

Feng Z, Pang J, Nouchi I, Kobayashi K, Yamakawa T, Zhu J (2010) Apoplastic ascorbate contributes to the differential ozone sensitivity in two varieties of winter wheat under fully open-air field conditions. Environ Pollut **158:** 3539–3545

Feng Z, Sun J, Wan W, Hu E, Calatayud V (2014) Evidence of widespread ozone-induced visible injury on plants in Beijing, China. Environ Pollut **193:** 296–301

Fiscus EL, Booker FL, Burkey KO (2005) Crop responses to ozone: uptake, modes of action, carbon assimilation and partitioning. Plant Cell Environ **28:** 997–1011

Floerl S, Majcherczyk A, Possienke M, Feussner K, Tappe H, Gatz C, Feussner I, Kües U, Polle A (2012) *Verticillium longisporum* infection affects the leaf apoplastic proteome, metabolome, and cell wall properties in *Arabidopsis thaliana*. PLoS One **7:** e31435

Frei M (2015) Breeding of ozone resistant rice: relevance, approaches and challenges. Environ Pollut **197:** 144–155

Frei M, Kohno Y, Wissuwa M, Makkar HPS, Becker K (2011) Negative effects of tropospheric ozone on the feed value of rice straw are mitigated by an ozone tolerance QTL. Glob Change Biol **17:** 2319–2329

Frei M, Tanaka JP, Chen CP, Wissuwa M (2010) Mechanisms of ozone tolerance in rice: characterization of two QTLs affecting leaf bronzing by gene expression profiling and biochemical analyses. J Exp Bot **61:** 1405–1417

Frei M, Tanaka JP, Wissuwa M (2008) Genotypic variation in tolerance to elevated ozone in rice: dissection of distinct genetic factors linked to tolerance mechanisms. J Exp Bot **59:** 3741–3752

Frei M, Wissuwa M, Pariasca-Tanaka J, Chen CP, Südekum KH, Kohno Y (2012) Leaf ascorbic acid level: is it really important for ozone tolerance in rice? Plant Physiol Biochem **59:** 63–70

Fridman E, Pichersky E (2005) Metabolomics, genomics, proteomics, and the identification of enzymes and their substrates and products. Curr Opin Plant Biol **8:** 242–248

Garchery C, Gest N, Do PT, Alhagdow M, Baldet P, Menard G, Rothan C, Massot C, Gautier H, Aarrouf J, et al (2013) A diminution in ascorbate oxidase activity affects carbon allocation and improves yield in tomato under water deficit. Plant Cell Environ **36:** 159–175

Hao D, Ohme-Takagi M, Sarai A (1998) Unique mode of GCC box recognition by the DNA-binding domain of ethylene-responsive element-binding factor (ERF domain) in plant. J Biol Chem **273:** 26857–26861

Heath MC (2000) Hypersensitive response-related death. Plant Mol Biol **44:** 321–334

Helmersson A, von Arnold S, Bozhkov PV (2008) The level of free intracellular zinc mediates programmed cell death/cell survival decisions in plant embryos. Plant Physiol **147:** 1158–1167

Hodges DM, DeLong JM, Forney CF, Prange RK (1999) Improving the thiobarbituric acid-reactive-substances assay for estimating lipid peroxidation in plant tissues containing anthocyanin and other interfering compounds. Planta **207:** 604–611

Hoegger PJ, Kilaru S, James TY, Thacker JR, Kües U (2006) Phylogenetic comparison and classification of laccase and related multicopper oxidase protein sequences. FEBS J **273:** 2308–2326

Höller S, Hajirezaei MR, von Wirén N, Frei M (2014a) Ascorbate metabolism in rice genotypes differing in zinc efficiency. Planta **239:** 367–379

Höller S, Meyer A, Frei M (2014b) Zinc deficiency differentially affects redox homeostasis of rice genotypes contrasting in ascorbate level. J Plant Physiol **171:** 1748–1756

Ishibashi Y, Tawaratsumida T, Zheng SH, Yuasa T, Iwaya-Inoue M (2010) NADPH oxidases act as key enzyme on germination and seedling growth in barley (*Hordeum vulgare* L.). Plant Prod Sci **13:** 45–52

Itzhaki H, Maxson JM, Woodson WR (1994) An ethylene-responsive enhancer element is involved in the senescence-related expression of the carnation glutathione-*S*-transferase (*GST1*) gene. Proc Natl Acad Sci USA **91:** 8925–8929

Jeon JS, Lee S, Jung KH, Jun SH, Jeong DH, Lee J, Kim C, Jang S, Yang K, Nam J, et al (2000) T-DNA insertional mutagenesis for functional genomics in rice. Plant J **22:** 561–570

Jeong DH, An S, Kang HG, Moon S, Han JJ, Park S, Lee HS, An K, An G (2002) T-DNA insertional mutagenesis for activation tagging in rice. Plant Physiol **130:** 1636–1644

Jeong DH, An S, Park S, Kang HG, Park GG, Kim SR, Sim J, Kim YO, Kim MK, Kim SR, et al (2006) Generation of a flanking sequence-tag database for activation-tagging lines in japonica rice. Plant J **45:** 123–132

Kangasjärvi J, Jaspers P, Kollist H (2005) Signalling and cell death in ozone-exposed plants. Plant Cell Environ **28:** 1021–1036

Kato N, Esaka M (2000) Expansion of transgenic tobacco protoplasts expressing pumpkin ascorbate oxidase is more rapid than that of wild-type protoplasts. Planta **210:** 1018–1022

Kawano T, Muto S (2000) Mechanism of peroxidase actions for salicylic acid-induced generation of active oxygen species and an increase in cytosolic calcium in tobacco cell suspension culture. J Exp Bot **51:** 685–693

Khokon AR, Okuma E, Hossain MA, Munemasa S, Uraji M, Nakamura Y, Mori IC, Murata Y (2011) Involvement of extracellular oxidative burst in salicylic acid-induced stomatal closure in *Arabidopsis*. Plant Cell Environ **34:** 434–443

Kitajima S, Koyama T, Yamada Y, Sato F (1998) Constitutive expression of the neutral PR-5 (OLP, PR-5d) gene in roots and cultured cells of tobacco is mediated by ethylene-responsive *cis*-element AGCCGCC sequences. Plant Cell Rep **18:** 173–179

Kojima S, Takahashi Y, Kobayashi Y, Monna L, Sasaki T, Araki T, Yano M (2002) *Hd3a*, a rice ortholog of the *Arabidopsis FT* gene, promotes transition to flowering downstream of *Hd1* under short-day conditions. Plant Cell Physiol **43:** 1096–1105

Lee MW, Qi M, Yang Y (2001) A novel jasmonic acid-inducible rice *myb* gene associates with fungal infection and host cell death. Mol Plant Microbe Interact **14:** 527–535

Libault M, Zhang XC, Govindarajulu M, Qiu J, Ong YT, Brechenmacher L, Berg RH, Hurley-Sommer A, Taylor CG, Stacey G (2010) A member of the highly conserved *FWL* (tomato *FW2.2-like*) gene family is essential for soybean nodule organogenesis. Plant J **62:** 852–864

Lima JC, Arenhart RA, Margis-Pinheiro M, Margis R (2011) Aluminum triggers broad changes in microRNA expression in rice roots. Genet Mol Res **10:** 2817–2832

Liso R, De Tullio MC, Ciraci S, Balestrini R, La Rocca N, Bruno L, Chiappetta A, Bitonti MB, Bonfante P, Arrigoni O (2004) Localization of ascorbic acid, ascorbic acid oxidase, and glutathione in roots of *Cucurbita maxima* L. J Exp Bot **55:** 2589–2597

Luwe M, Takahama U, Heber U (1993) Role of ascorbate in detoxifying ozone in the apoplast of spinach (*Spinacia oleracea* L.) leaves. Plant Physiol **101:** 969–976

Maggs R, Ashmore MR (1998) Growth and yield responses of Pakistan rice (*Oryza sativa* L.) cultivars to O_3 and NO_2. Environ Pollut **103:** 159–170

Matsushita A, Inoue H, Goto S, Nakayama A, Sugano S, Hayashi N, Takatsuji H (2013) Nuclear ubiquitin proteasome degradation affects WRKY45 function in the rice defense program. Plant J **73:** 302–313

McGuirl MA, Dooley DM (1999) Copper-containing oxidases. Curr Opin Chem Biol **3:** 138–144

Miller JD, Arteca RN, Pell EJ (1999) Senescence-associated gene expression during ozone-induced leaf senescence in Arabidopsis. Plant Physiol **120:** 1015–1024

Omasa K, Tobe K, Kondo T 2002. Absorption of organic and inorganic air pollutants by plants. *In* K Omasa, H Saji, S Youssefian, N Kondo, eds, Air Pollution and Plant Biotechnology. Springer, Tokyo, pp 155–178

Overmyer K, Brosché M, Kangasjärvi J (2003) Reactive oxygen species and hormonal control of cell death. Trends Plant Sci **8:** 335–342

Overmyer K, Kollist H, Tuominen H, Betz C, Langebartels C, Wingsle G, Kangasjärvi S, Brader G, Mullineaux P, Kangasjärvi J (2008) Complex phenotypic profiles leading to ozone sensitivity in *Arabidopsis thaliana* mutants. Plant Cell Environ **31:** 1237–1249

Overmyer K, Tuominen H, Kettunen R, Betz C, Langebartels C, Sandermann H Jr, Kangasjärvi J (2000) Ozone-sensitive *Arabidopsis rcd1* mutant reveals opposite roles for ethylene and jasmonate signaling pathways in regulating superoxide-dependent cell death. Plant Cell **12:** 1849–1862

Pennell RI, Lamb C (1997) Programmed cell death in plants. Plant Cell **9:** 1157–1168

Petersen TN, Brunak S, von Heijne G, Nielsen H (2011) SignalP 4.0: discriminating signal peptides from transmembrane regions. Nat Methods **8:** 785–786

Pignocchi C, Fletcher JM, Wilkinson JE, Barnes JD, Foyer CH (2003) The function of ascorbate oxidase in tobacco. Plant Physiol **132:** 1631–1641

Pignocchi C, Foyer CH (2003) Apoplastic ascorbate metabolism and its role in the regulation of cell signalling. Curr Opin Plant Biol **6:** 379–389

Plöchl M, Lyons T, Ollerenshaw J, Barnes J (2000) Simulating ozone detoxification in the leaf apoplast through the direct reaction with ascorbate. Planta **210:** 454–467

Porra RJ, Thompson WA, Kriedemann PE (1989) Determination of accurate extinction coefficients and simultaneous equations for assaying chlorophylls *a* and *b* extracted with four different solvents: verification of the concentration of chlorophyll standards by atomic absorption spectroscopy. Biochim Biophys Acta **975:** 384–394

Pourcel L, Routaboul JM, Kerhoas L, Caboche M, Lepiniec L, Debeaujon I (2005) *TRANSPARENT TESTA10* encodes a laccase-like enzyme involved in oxidative polymerization of flavonoids in *Arabidopsis* seed coat. Plant Cell **17:** 2966–2980

Rao MV, Davis KR (2001) The physiology of ozone induced cell death. Planta **213:** 682–690

Rao MV, Lee H, Creelman RA, Mullet JE, Davis KR (2000) Jasmonic acid signaling modulates ozone-induced hypersensitive cell death. Plant Cell **12:** 1633–1646

Rao MV, Lee HI, Davis KR (2002) Ozone-induced ethylene production is dependent on salicylic acid, and both salicylic acid and ethylene act in concert to regulate ozone-induced cell death. Plant J **32:** 447–456

Saitou N, Nei M (1987) The neighbor-joining method: a new method for reconstructing phylogenetic trees. Mol Biol Evol **4:** 406–425

Sakai H, Lee SS, Tanaka T, Numa H, Kim J, Kawahara Y, Wakimoto H, Yang CC, Iwamoto M, Abe T, et al (2013) Rice Annotation Project Database (RAP-DB): an integrative and interactive database for rice genomics. Plant Cell Physiol **54:** e6

Sanmartin M, Drogoudi PA, Lyons T, Pateraki I, Barnes J, Kanellis AK (2003) Over-expression of ascorbate oxidase in the apoplast of transgenic tobacco results in altered ascorbate and glutathione redox states and increased sensitivity to ozone. Planta **216:** 918–928

Sato F, Kitajima S, Koyama T, Yamada Y (1996) Ethylene-induced gene expression of osmotin-like protein, a neutral isoform of tobacco PR-5, is mediated by the AGCCGCC *cis*-sequence. Plant Cell Physiol **37:** 249–255

Sato Y, Antonio BA, Namiki N, Takehisa H, Minami H, Kamatsuki K, Sugimoto K, Shimizu Y, Hirochika H, Nagamura Y (2011) RiceXPro: a platform for monitoring gene expression in *japonica* rice grown under natural field conditions. Nucleic Acids Res **39:** D1141–D1148

Sawada H, Kohno Y (2009) Differential ozone sensitivity of rice cultivars as indicated by visible injury and grain yield. Plant Biol (Suppl 1) **11:** 70–75

Shah KH, Almaghrabi B, Bohlmann H (2013) Comparison of expression vectors for transient expression of recombinant proteins in plants. Plant Mol Biol Rep **31:** 1529–1538

Shimono M, Sugano S, Nakayama A, Jiang CJ, Ono K, Toki S, Takatsuji H (2007) Rice WRKY45 plays a crucial role in benzothiadiazole-inducible blast resistance. Plant Cell **19:** 2064–2076

Takahashi Y, Teshima KM, Yokoi S, Innan H, Shimamoto K (2009) Variations in Hd1 proteins, *Hd3a* promoters, and *Ehd1* expression levels contribute to diversity of flowering time in cultivated rice. Proc Natl Acad Sci USA **106:** 4555–4560

Tamura K, Peterson D, Peterson N, Stecher G, Nei M, Kumar S (2011) MEGA5: molecular evolutionary genetics analysis using maximum likelihood, evolutionary distance, and maximum parsimony methods. Mol Biol Evol **28:** 2731–2739

Tani T, Sobajima H, Okada K, Chujo T, Arimura S, Tsutsumi N, Nishimura M, Seto H, Nojiri H, Yamane H (2008) Identification of the *OsOPR7* gene encoding 12-oxophytodienoate reductase involved in the biosynthesis of jasmonic acid in rice. Planta **227:** 517–526

Tilman D, Balzer C, Hill J, Befort BL (2011) Global food demand and the sustainable intensification of agriculture. Proc Natl Acad Sci USA **108:** 20260–20264

Turcsányi E, Lyons T, Plöchl M, Barnes J (2000) Does ascorbate in the mesophyll cell walls form the first line of defence against ozone? Testing the concept using broad bean (*Vicia faba* L.). J Exp Bot **51:** 901–910

Ueda Y, Frimpong F, Qi Y, Matthus E, Wu L, Höller S, Kraska T, Frei M (2015) Genetic dissection of ozone tolerance in rice (*Oryza sativa* L.) by a genome-wide association study. J Exp Bot **66:** 293–306

Ueda Y, Uehara N, Sasaki H, Kobayashi K, Yamakawa T (2013a) Impacts of acute ozone stress on superoxide dismutase (SOD) expression and reactive oxygen species (ROS) formation in rice leaves. Plant Physiol Biochem **70:** 396–402

Ueda Y, Wu L, Frei M (2013b) A critical comparison of two high-throughput ascorbate analyses methods for plant samples. Plant Physiol Biochem **70:** 418–423

Vahisalu T, Kollist H, Wang YF, Nishimura N, Chan WY, Valerio G, Lamminmäki A, Brosché M, Moldau H, Desikan R, et al (2008) SLAC1 is required for plant guard cell S-type anion channel function in stomatal signalling. Nature **452:** 487–491

Van Dingenen R, Dentener FJ, Raes F, Krol MC, Emberson L, Cofala J (2009) The global impact of ozone on agricultural crop yields under current and future air quality legislation. Atmos Environ **43:** 604–618

Wang X, Manning W, Feng Z, Zhu Y (2007) Ground-level ozone in China: distribution and effects on crop yields. Environ Pollut **147:** 394–400

Wang Y, Frei M (2011) Stressed food: the impact of abiotic environmental stresses on crop quality. Agric Ecosyst Environ **141:** 271–286

Wang Y, Yang L, Höller M, Zaisheng S, Pariasca-Tanaka J, Wissuwa M, Frei M (2014) Pyramiding of ozone tolerance QTLs *OzT8* and *OzT9* confers improved tolerance to season-long ozone exposure in rice. Environ Exp Bot **104:** 26–33

Wissuwa M, Ismail AM, Yanagihara S (2006) Effects of zinc deficiency on rice growth and genetic factors contributing to tolerance. Plant Physiol **142:** 731–741

Wohlgemuth H, Mittelstrass K, Kschieschan S, Bender J, Weigel HJ, Overmyer K, Kangasjärvi J, Sandermann H, Langebartels C (2002) Activation of an oxidative burst is a general feature of sensitive plants exposed to the air pollutant ozone. Plant Cell Environ **25:** 717–726

Yamada S, Kano A, Tamaoki D, Miyamoto A, Shishido H, Miyoshi S, Taniguchi S, Akimitsu K, Gomi K (2012) Involvement of OsJAZ8 in jasmonate-induced resistance to bacterial blight in rice. Plant Cell Physiol **53:** 2060–2072

Yamaji K, Ohara T, Uno I, Kurokawa J, Pochanart P, Akimoto H (2008) Future prediction of surface ozone over east Asia using Models-3 Community Multiscale Air Quality Modeling System and Regional Emission Inventory in Asia. J Geophys Res **113:** D08306

Yamaji K, Ohara T, Uno I, Tanimoto H, Kurokawa J, Akimoto H (2006) Analysis of the seasonal variation of ozone in the boundary layer in East Asia using the Community Multi-scale Air Quality model: what controls surface ozone levels over Japan? Atmos Environ **40:** 1856–1868

Yamamoto A, Bhuiyan MNH, Waditee R, Tanaka Y, Esaka M, Oba K, Jagendorf AT, Takabe T (2005) Suppressed expression of the apoplastic ascorbate oxidase gene increases salt tolerance in tobacco and *Arabidopsis* plants. J Exp Bot **56:** 1785–1796

Yoshida S, Forno DA, Cock JH, Gomez KA 1976. Laboratory Manual for Physiological Studies of Rice. International Rice Research Institute, Manila, The Philippines

Yu D, Chen C, Chen Z (2001) Evidence for an important role of WRKY DNA binding proteins in the regulation of *NPR1* gene expression. Plant Cell **13:** 1527–1540